MIMO Digital Signal Processing in Few-Mode Fiber Optical Communication Systems

A Dissertation

Presented to the

Graduate Faculty of the

University of Louisiana at Lafayette

In Partial Fulfillment of the

Requirements for the Degree

Doctor of Philosophy

Xuan He

Fall 2014

ProQuest LLC.
789 East Eisenhower Parkway
P.O. Box 1346
Ann Arbor, MI 48106 - 1346

MIMO Digital Signal Processing in Few-Mode Fiber Optical Communication Systems

Xuan He

APPROVED:

Zhongqi Pan, Chair Professor of Electrical and Computer Engineering	Hongyi Wu Professor of Computer Science The Center for Advanced Computer Studies
Dmitri Perkins Professor of Computer Science The Center for Advanced Computer Studies	Magdy Bayoumi Professor of Computer Engineering The Center for Advanced Computer Studies
Mary Farmer-Kaiser Interim Dean of the Graduate School	

ACKNOWLEDGMENTS

First of all, I would like to sincerely express gratitude to my advisor, Prof. Zhongqi Pan, for the continuous support on my Ph.D study. I am very fortunate to have his guidance. Whenever I have difficulties in my research, he is always patient and enthusiastic to help me. Prof. Pan also gave me a hand in seeking summer internships every year. Thanks for all his help, which makes me live an extraordinary life and have fruitful research results in the last five years.

Thanks for Dr. Hongyi Wu. It was a very great experience in attending his weekly group seminar, which extensively expanded my knowledge on advanced wireless communication technologies. Thanks for Dr. Perkins. His course taught me a lot on advanced wireless communication protocols. I would also thank Dr. Bayoumi. I learned much knowledge and hands-on experience in hardware design from his courses.

My thanks also goes to Dr. Xiang Zhou at Google.Inc. It was a very exciting experience working with him at AT&T Lab-research in summer, 2012. Thanks for Dr. Bo Zhang at Juniper Networks for his mentoring on my internship in summer 2013 and summer 2014.

I will never forget our optical research group members: Dr. Junyi Wang, Mr. Yi Weng, Ms. Lu Yang, and Mr. Kailu Gao. Thanks for their help on both my research and daily life. Thanks for Mr. Shelby William at Electrical and Computer Engineering Department. He helped me a lot on solving the IT problems in the lab.

Last but not least, my deepest thanks to my wife, Bing Chao and my parents, Mingzhong He and Li Li. They are always my biggest support!

TABLE OF CONTENTS

LIST OF TABLES

LIST OF FIGURES

LIST OF ABBREVIATIONS

ADC	Analog to digital converter
ASE	Amplified stimulated emission noise
BER	Bit-error rate
CD	Chromatic dispersion
CMA	Constant modulus algorithm
DMGD	Differential mode group delay
DSP	Digital signal processing
DSF	Dispersion shifted fiber
EDFA	Erbium doped fiber amplifier
E/O	Electrical to optical conversion
FD	Frequency domain
FMF	Few-mode fiber
FFT	Fast Fourier transform
ISI	Inter-symbol interference
LO	Local oscillator
LMS	Least mean square
MMF	Multi-mode fiber
MIMO	Multi-input multi-output
MCF	Multi-core fiber
MDL	Mode dependent loss
MDG	Mode dependent gain
O/E	Optical to electrical conversion

OSNR	Optical signal-to-noise ratio
PMD	Polarization mode dispersion
PSD	Power spectral density
PDM	Polarization division multiplexing
SDM	Space division multiplexing
SISO	Single-input single-output
S/P	Serial to parallel
TD	Time domain
WDM	Wavelength-division multiplexing

CHAPTER 1: INTRODUCTION

Space-division multiplexing (SDM) has emerged as a next-generation technology to sustain the continuous traffic growth, in order to keep up with the future of Internet bandwidth requirement [1]. Among SDM technologies, SDM using few-mode fiber (FMF) transmission has been extensively explored [2-10]. Since the conventional multi-mode fiber (MMF) is not suitable for long distance SDM transmission because of its very large differential mode group delay (DMGD) and more than hundreds of spatial modes, the few-mode fiber is developed with only the support of small number of spatial modes at relatively small DMGD [11].

In FMF transmission systems, each data channel is modulated onto individual spatial or polarization mode to increase the overall number of parallel channels, thus enabling higher transmission capacity. One of the fundamental challenges in FMF transmission systems is the random inter-modal crosstalk between any two spatial or polarization modes. Another significant challenge is the large accumulated DMGD, which can induce significant inter-symbol interference (ISI) on each spatial mode signal in SDM systems.

Many research articles have demonstrated that, with digital signal processing (DSP), the adaptive multi-input multi-output (MIMO) equalizer can dynamically compensate DMGD and untangle the spatial modes [12-14]. The large accumulated DMGD and a number of spatial channels need very complex DSP hardware for MIMO processing [15]. The number of single-input single-output (SISO) equalizers, which compose the MIMO equalizer, grows quadratically with the number of spatial channels, and the tap number of every SISO equalizer is linearly increased with the accumulated DMGD in FMF systems.

Among several adaptive MIMO equalization methods, least mean square (LMS) approach is considered as the most attractive one, for it is a good compromise among equalization performance, hardware complexity, and dynamic speed. The adaptive LMS based MIMO equalizer can be either implemented in the time domain (TD) or frequency domain (FD). By taking advantage of fast Fourier transform (FFT) and block-based equalization, the adaptive frequency domain method can achieve much lower hardware complexity in compensating the large accumulated DMGD in the FMF transmission systems [16-19]. Several experimental results have also confirmed better hardware efficiency of the frequency domain approach [19-21].

As in the single-mode fiber transmission systems, chromatic dispersion (CD) is another linear impairment, which needs to be compensated before spatial de-multiplexing in FMF transmission systems. In conventional DSP, two-stage equalization architecture is usually used, which compensates the CD by a static FDE in the first stage and compensates DMGD by an adaptive frequency domain MIMO equalizer in the second stage. The conventional two-stage architecture is the most hardware efficient approach in normal single-mode fiber systems, which requires CD and polarization mode dispersion (PMD) compensation separately, because the PMD is much lower than CD. However, in FMF systems, the DMGD is usually larger than CD, such that the same adaptive MIMO equalizer used for DMGD compensation can also be used for CD compensation without increasing the filter tap length, thus eliminate the need for an independent CD compensation module. Such a single-stage adaptive equalizer could greatly reduce the DSP implementation complexity for FMF transmission systems, and can also enable the dynamic routing optical networks, in which the link CD is unknown [22, 23].

In addition to the hardware complexity, the convergence speed of adaptive MIMO equalizer is another key consideration, which may significantly impact the system efficiency. In FMF systems, the periodical training sequence is usually used for the channel estimation. Because the dynamic change of FMF channel, a decision-directed adaptive approach is switched on after initial channel estimation. With such equalizer architecture, slower convergence speed of the adaptive MIMO equalizer may require a longer training sequence in the system for its initial channel estimation, thus decreasing the overall system efficiency.

In both TD-LMS and FD-LMS MIMO equalizers, the parameter of step size controls both equalization performance and convergence speed. In the conventional FD-LMS equalizer, a same step size are chosen for all frequency bins and it keeps constant during channel estimation. Generally, the larger step size can achieve faster convergence speed but also results in more residual penalty after equalization.

To increase the convergence rate while keeping the same equalization performance, a signal power spectrum density (PSD) dependent method and a noise PSD directed method are proposed and compared [24, 25]. The signal PSD dependent method can effectively increase the convergence speed over the conventional adaptive FD-LMS method with negligible hardware complexity increase. The signal PSD dependent approach adopts variable step size overall frequency bins of FFT blocks inverse to its power level, which enables the estimation error of each frequency bin converges to zero. However, the PSD dependent method does not consider the system background noise, so it is only an optimum solution in noise-free channels. In the noise PSD directed adaptive FD-LMS algorithm, the frequency bin-wise step size of each FFT block is chosen to make posterior error of each frequency bin converge to the background noise in the FMF system with additive white

Gaussian noise (AWGN) channel, where the noise bins can be iteratively estimated with knowledge of input signal power spectrum, error vector spectrum and their cross-correlation spectrum.

In the real optical systems, the finite linewidth of both transmitter laser and local oscillator (LO) will induce the phase noise, which needs to be estimated. In the single-mode fiber systems with QPSK modulation, the constant-modulus algorithm (CMA) is used for blind adaptive equalization, which does not require the phase estimation before adaptive equalization. However, in FMF systems with a larger number of channels and large accumulated DMGD, the training sequence will be used for adaptive channel estimation. In such equalizer architecture, the phase noise may significantly affect the feedback errors for adaptive equalizer updates. The proposed fast convergent algorithm uses the M^{th} power phase estimation in the feedback loop to mitigate the effect of phase noise on the performance of MIMO equalizer [26].

In the presence of mode dependent gain (MDG) of FMF amplifiers and mode dependent loss (MDL) of FMF, the simulation results will show that the proposed method can keep the same convergence speed, while some channels with bigger loss may have more penalty after equalization.

The rest of the dissertation is organized as follows: Chapter 2 will introduce the evolution of optical communication systems and architecture of few-mode fiber optical communication systems. Chapter 3 will show introduce and compare different SDM technologies. Chapter 4 will talk about the FMF systems and the system impairments. Chapter 5 will introduce and compare the conventional MIMO equalization methods: adaptive TD-LMS and adaptive FD-LMS MIMO equalization. Chapter 6 will present our proposed low hardware complexity single-stage MIMO equalizer. Chapter 7 will introduce our proposed two fast convergent step

size controlled FD-LMS algorithms. Chapter 8 will apply the proposed fast convergent method to increases the convergence rate of single-stage MIMO equalizer. Chapter 9 will conclude the dissertation.

CHAPTER 2: EVOLUTION OF OPTICAL COMMUNICATION SYSTEMS

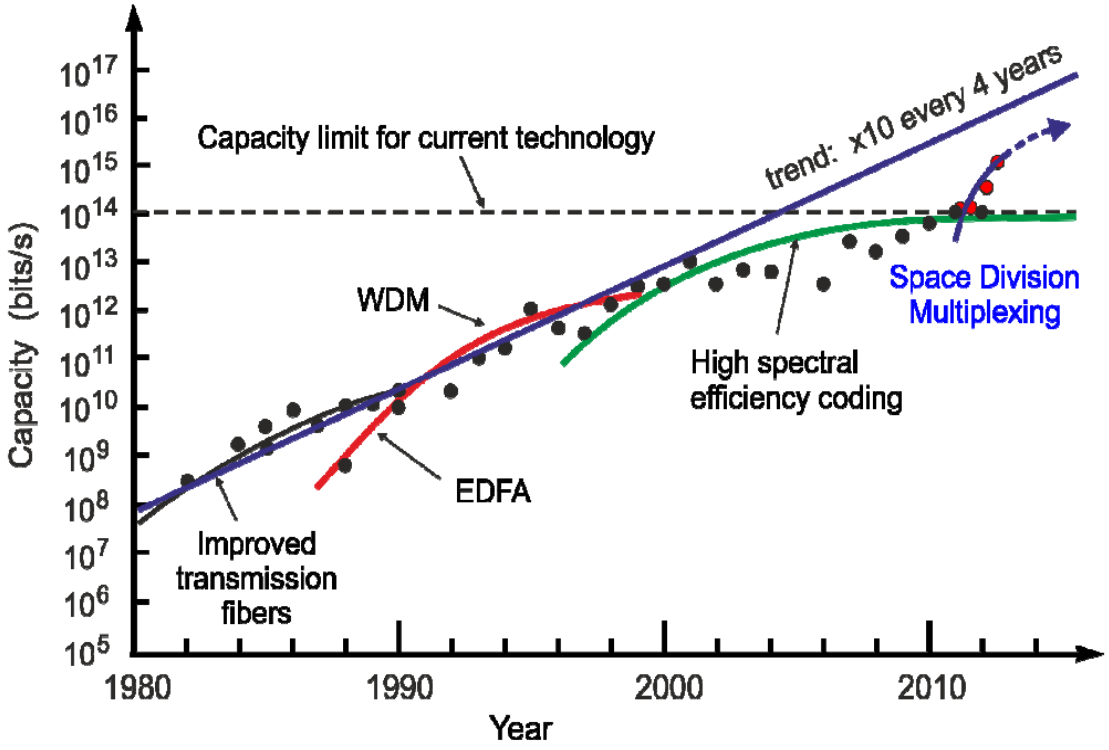

Figure 1. Evolution of optical communication technology

Figure. 1 shows the evolution of optical fiber communication systems driven by continuous technological breakthroughs, including the low-loss and dispersion-shifted single-mode fiber, the Erbium Doped Fiber Amplifier (EDFA), the wavelength-division multiplexing (WDM), and the high spectral efficiency coding enabled by the coherent detection and DSP [1]. Every point of Figure 1 records the highest transmission capacity reported in the corresponding year Optical Communication Conference (OFC).

As early as 1966, Charles Kao first demonstrated that the glass fiber can be used as a medium to transmit signals and predicted that the attenuation limit of glass fibers for transmission should be below 20 dB/km. After 4 years of his proposal, the fiber with 20 dB/km was achieved by Kapron, etc. During the 1970s, the low-loss fibers were constantly

evolved and reported. For example, below 5 dB/km at 850 nm low loss fiber was reported in 1973, and in 1979, the fiber with ultra-low loss of 0.2 dB/km at 1550nm was reported by T. Miya, etc., which is the standard attenuation of current deployed single mode fibers.

In the 1980s, it was observed that the wavelength with lowest fiber attenuation is at 1550 nm, but the lowest fiber CD is at 1310 nm. In order to achieve the lowest fiber loss and chromatic dispersion, the dispersion-shifted fiber (DSF) was developed. At that time, frequent optical to electrical conversion (O/E), electrical regeneration, and electrical to optical conversion (E/O) were highly needed to amplify the signals along fiber transmission. Until the late 1980s, the invention of advanced EDFA, another milestone of optical communication, help to realize the all-optical amplification, thus enabling longer transmission distance with lower system cost.

In the mid 1990s, the disruptive technology of WDM was introduced following the EDFA. The WDM technology can transmit multiple channels in one fiber, which revealed a larger fiber capacity than ever before. It also helped the service carrier with the simplest and most cost effective system upgrade by only adding new channels at fiber two ends. In the same period, the broadband EDFA was developed to support the amplification of WDM channels over transmission band. Other optical components, like optical filter, wavelength multiplexer/de-multiplexer, etc., were extensively developed to provide necessary functions to the systems. Later on, dense wavelength division multiplexing with smaller channel spacing was seamlessly introduced after initial WDM to enlarge higher transmission capacity.

From the mid 2000s, coherent detection started attracting attention as the way to sustain the exponential traffic growth following WDM technology because it allows the signals

modulated on both amplitude and phase of optical carriers. The coherent detection was first proposed as early as the 1970s to detect the optical signal. However, because intensity (ID) modulation was widely used and direct detection (DD) can simply detect the 1s or 0s bits, it did not attract any attention for its higher complexity. In the 1980s, coherent detection was re-investigated to achieve higher receiver sensitivity with local oscillator amplification, but the invention of EDFA quickly took over that role. Until recent years, coherent detection in combination with DSP served as the key technique to support higher transmission capacity of each WDM channel, as it allows high modulation formats, polarization multiplexing, and importantly enables electrical mitigation of signal distortion with cost effective DSP other than complex optical components. In coherent systems, the demodulated signals after coherent detection are re-sampled by high-speed analog-to-digital converter (ADC), and then several DSP functions are used to do carrier recovery and compensate the signal distortion, like polarization de-multiplexing, chromatic dispersion compensation, polarization mode dispersion compensation, and so on.

In Figure 1, it predicts that that the maximum capacity of single-mode fiber systems should be no more than 100 Tb/s with transmission and amplification of signals over the full C+L bands at 10 bits/s/Hz spectral efficiency. So, it is extremely urgent for both academia and industries to find the next-generation technology to sustain the future bandwidth requirements as it exponentially grows. It is believed that exploitation of spatial dimension of optical fibers is the most promising way, which can also be learned from Figure 2 [27], which shows all the available multiplexing dimensions in optical fiber systems including frequency dimension, polarization dimension, amplitude dimension, phase dimension, and spatial dimension.

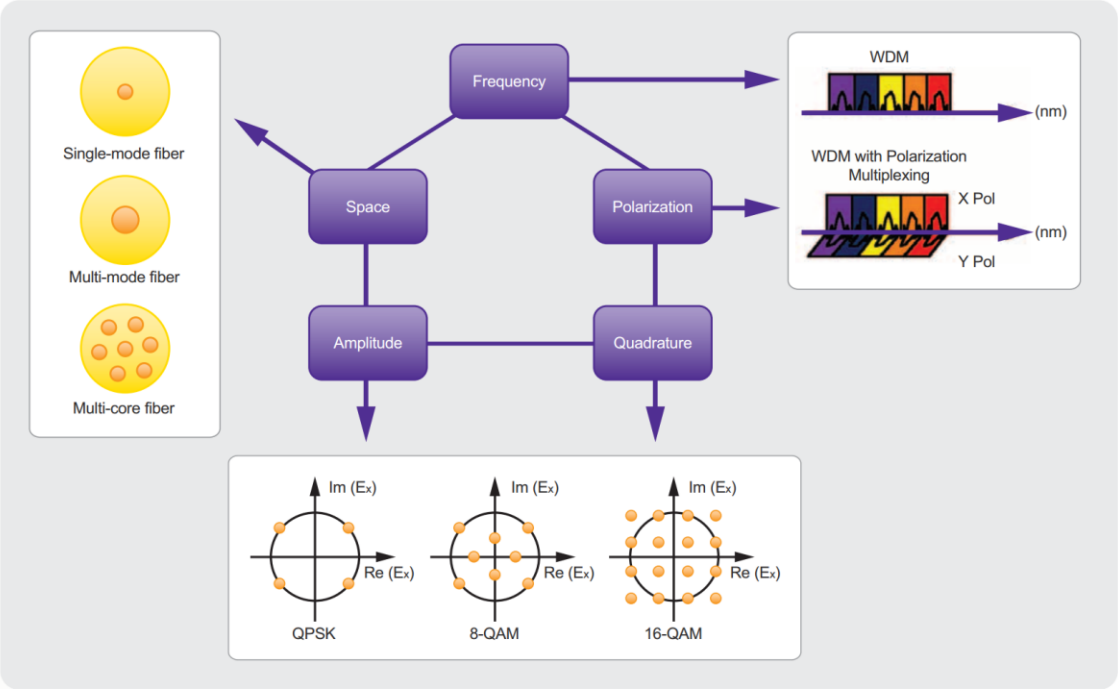

Figure 2. Multiplex dimensions of optical communication systems

In DWDM systems, the frequency dimension is intensively taken advantage of to transmit signals over multiple wavelength channels. In high spectral efficiency coding, the polarization, amplitude and phase of optical carriers are used to enable a higher bit rate of each WDM channel. As in latest commercial optical systems, the polarization-division multiplexing (PDM) QPSK signals and PDM-16-QAM signals are already used for 100G and 400G optical transmission. Although very high-level modulation formats, like 64-QAM, 128-QAM, etc., can provide very high spectral efficiency, it has very low noise tolerance, thus considerably limiting the transmission distance. So, only the space dimension is not fully exploited. The figure shows three fiber types for SDM technology: bundled single-mode fiber, FMF and multi-core fiber (MCF).

CHAPTER 3: SDM OPTICAL COMMUNICATION SYSTEMS

3.1 Architecture of SDM systems

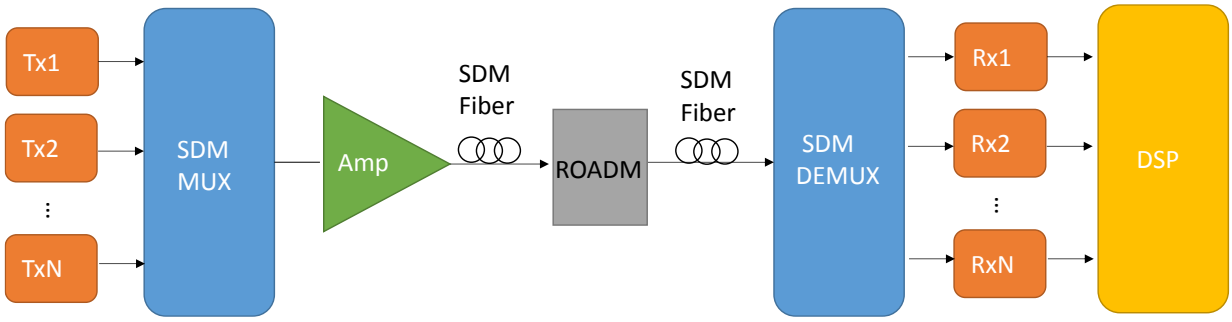

Figure 3. Architecture of SDM systems

As early as 1970, the concept of SDM was proposed to transmit signals over multiple fiber cores, but the crosstalk between any two cores cannot be finely controlled. Until recently, as the predicted capacity crunch of single-mode fiber for rapidly growing traffic, SDM technology is re-considered as the promising way to sustain the bandwidth requirement in future decades. On one side, the manufactural progress of optical components, like specialized design of large DMGD or low crosstalk MMF, fine fabrication control of multi-core or hollow-core fiber, and specialized mode generator and so on. On the other side, the development of coherent technology together with DSP enable to solve the unique crosstalk and distortions with MIMO processing.

As shown in Figure 3, N optical channels are spatially multiplexed with Mode multiplexer (MUX) and transmitted through SDM fibers. After fiber transmission, the mode de-multiplexed (DEMUX) is used to separate the N spatial channels. Since most of MUX and DEMUX are still free space devices, they can induce significant power loss and mode

coupling. There have been proposed different types of SDM fibers including bundled SMF, FMF, and MCF. The inter-modal crosstalk and link modal dispersion varies by the fiber type. For the FMF systems, there is very large DMGD and strong mode coupling between spatial modes. After DEMUX, the signals on spatial channels are coherently detected, and a N×N MIMO DSP is used to mitigate the signals crosstalk and distortion, like CD and DMGD. In the SDM systems, optical add and drop multiplexer can be used to dynamically add or drop necessary spatial channels at each network node to support the all-optical dynamic routing networks.

3.2 Comparison of Different SDM technologies

Several SDM fibers have been developed to support SDM transmission in optical systems as shown in Figure 4 [1]. (a) shows the fiber bundle made up by physically independent parallel single-mode fibers. Although the bundle may achieve higher fibers densities than current fiber cables by advanced design of fiber cladding, it cannot actually decrease the cost-per-bit for the system capacity, and costs are linearly increased with the number of fibers in the bundle.

(b) shows the multi-core fiber composed of independent single-mode cores in one fiber. The most challenging design of multi-core fiber is the control of crosstalk between any two cores. The core distance and core profile should be carefully designed to minimize the crosstalk. Ideally, the larger core distance, the less crosstalk occurs. However, growth of the number of cores or core distance increase the overall diameter of multi-core fiber, and the fiber is susceptible to fracture. Therefore, the overall capacity of multi-core fiber may be limited by the number of cores. Another challenge of multi-core fiber is the optical

integration. Because signals are transmitted through physically independent cores, it is difficult to share the pump power for different cores in multi-core fiber EDFA.

(c) shows the multi-mode fibers (MMF), which can support transmission of multiple channels over multiple spatial modes. Because all signals are transmitted in the same physical area, there is inevitable inter-model crosstalk. The current commercial MMF supports hundreds of spatial modes, but there are extreme large DMGD in ns/km, which is not compensated with DSP in practice. To take advantage of MMF in SDM, FMF was developed with only a small number of spatial modes. For example, state-of-the-art FMF can maximally support 3 spatial modes, including LP_{01}, LP_{11a}, and LP_{11b}. It has been prove that the MIMO DSP can be used to compensate the DMGD and inter-modal crosstalk in FMF systems. With progress of DSP in the future, it is believed that more spatial modes will be supported in FMF system. Also, many integrated optical components, like FMF EDFA, have been investigated to make it a stronger to candidate in SDM technology. It is predictable that, with the advantage of optical integration, the FMF system can achieve efficiency in both system cost and power consumption.

(d) shows the coupled multi-core fiber with larger core density than (b), and has the same problem in optical integration. (e) shows the photonic band gap fiber with ultra-low loss. Although it does not support SDM transmission, work is undergoing to see its potential in SDM systems. Therefore, with potential of capacity scalability and nature of optical integration, SDM technology using FMF can be an auspicious way to sustain next capacity crunch.

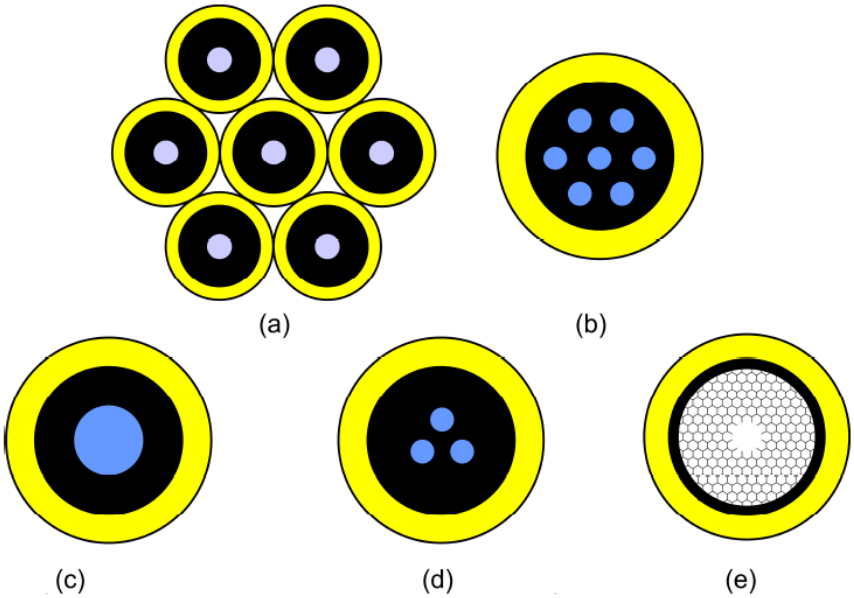

Figure 4. SDM fibers or cables

Figure. 5 shows the normalized propagation constant as a function of normalized frequency V for different spatial modes in the step-index MMF []. V is as follows:

$$V = kn\alpha \cdot \mathrm{sqrt}(2\Delta) \tag{3.1}$$

where, k equals to 2pi/λ, λ is wavelength, n is the refractive index of the core and α is core diameter. Δ is the numeric aperture determined by the refractive index difference between core and cladding. The figure shows the cutoff frequency of several spatial modes. For example, the cutoff frequency for LP_{01} and LP_{11} modes are 0 and 2.405, respectively. When the fiber normalized frequency is greater than the cutoff frequency of certain modes, those modes can be transmitted. So, the normalized frequency of commonly used 3 spatial modes FMF (LP_{01}, LP_{11a} and LP_{11b}) should be located in the range between 2.405 and 3.832. From the equation (1), the fiber normalized frequency or supported spatial modes can be designed by choosing fiber refractive index and core diameter.

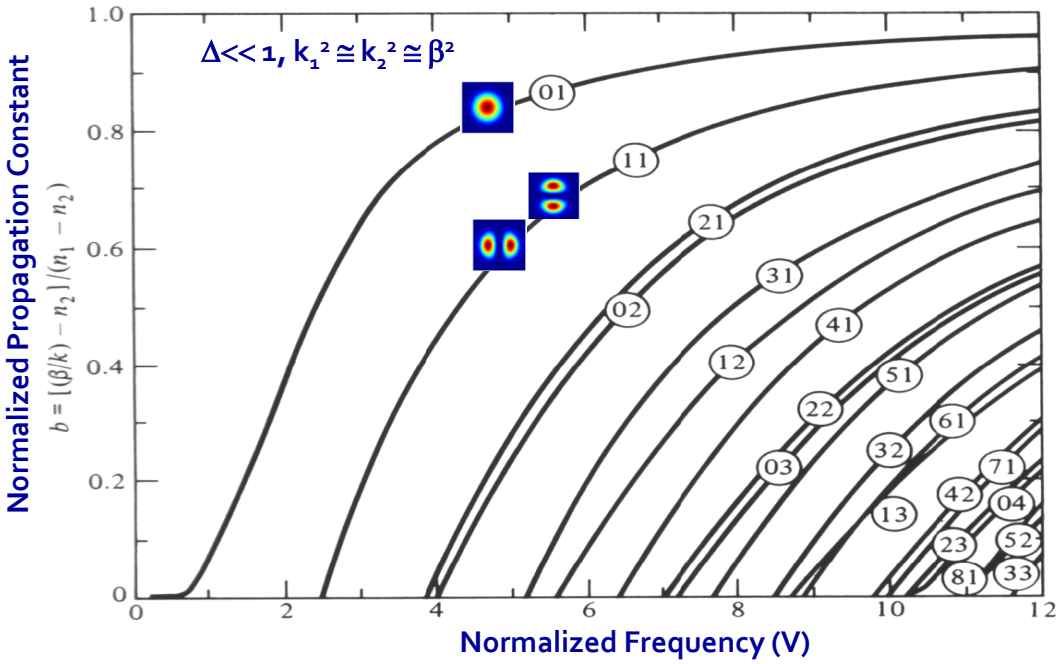

Figure 5. Normalized propagation constants of spatial modes in MMF

Table 1 comprehensively compared three fiber or cable types for SDM transmission: bundled SMF, MCF, and FMF. Because the MMF needs to support numerous spatial modes, which requires larger fiber numerical aperture, it may have very low loss in fusion splicing, which can save more link budget on SDM transmission. Because all spatial modes share the same transmission media, there is inevitable inter-modal crosstalk between any two spatial or polarization modes. In addition, because the spatial modes are transmitted at different propagation constant, as shown in Figure 5, there is large accumulated DMGD. The DMGD together with mode coupling can induce the ISI on every spatial mode during transmission. Although the cores in MCF are physically independent, the power coupling between separate cores is inevitable. The MIMO processing in DSP is needed to combat the DMGD and mode coupling in MCF and FMF. Since the core of FMF has a larger area than the cores in MCF and bundled SMF, it can achieve lower nonlinear threshold, which is another benefit that

makes FMF suitable for long-haul SDM transmission. The physically independent fiber cores of bundled SMF and MCF needs a number of ROADM and amplifier to service all cores in the transmission link, which not only increases the system cost, but also make the system upgrade harder. In the contrast, only one ROADM and amplifier can service all spatial modes, which means the system capacity can be easily upgraded without adding new amplifier or ROADM.

Table 1 Comparison of different SDM technologies

Parameter	Bundled SMF	MCF	FMF
Fiber loss	Standard	As low as SMF	As low as SMF
Effective area	Standard	Small or Standard	Large
Intra-mode nonlinearity	Standard	Standard or high	Low
Inter-mode nonlinearity	No	Low	Low to medium
Mode coupling crosstalk	No	Medium	Low to high, can be optimized
No. of amplifiers	N	N	1
No. of ROADM	N	N	1
Fusion splicing	Easy	Special splicer, Probably high loss	Easy, low loss
DSP complexity	Low	Low to medium	Medium to high
Cost	N*SMF	1*SMF	1*SMF
Application	Interconnect & long reach	Interconnect & long reach	Long reach

CHAPTER 4: FEW-MODE FIBER OPTICAL COMMUNICATION SYSTEMS

4.1 Architecture of FMF communication systems

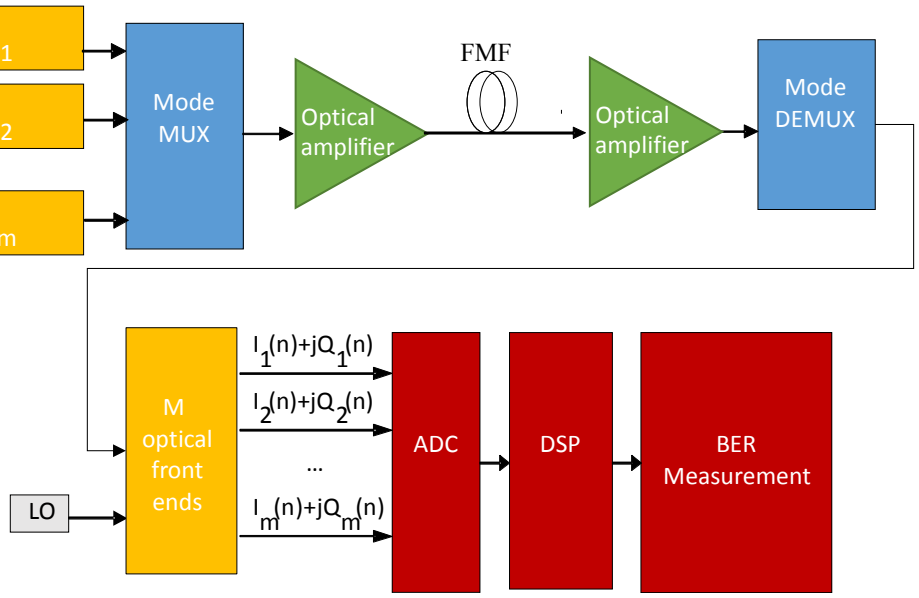

Figure 6. Conceptual diagram of FMF transmission systems

Figure 6 shows the concept of the M-mode FMF transmission system. The state-of-the-art transponder can transmit polarization multiplexed high spectral efficiency modulation formats at 28GSymbol/s data rate, like PDM-QPSK, PDM-16-QAM and so on. Most of the current FMF transmission experiments are based 100 Gbit/s (28G or 32G symbol rate) PDM-QPSK modulation format. The mode multiplexer is used to combine the spatial modes into the FMF, and the mode de-multiplexer is used to separate the spatial modes after transmission. Both mode MUX and DEMUX can induce large power loss as well as additional mode coupling. Along the transmission, the few-mode fibers will induce CD (≈ 20 ps/nm/km), large DMGD (up to 75 ps/km) and random inter-modal crosstalk. Few-mode optical amplifiers, like FMF EDFA, are used to compensate the fiber loss along transmission.

Except for signals amplification, the FMF amplifiers also induce the amplified stimulated emission (ASE) noise, which will significantly degrade the optical signal-to-noise ratio (OSNR). The FMF amplifier may additionally induce MDG.

After the receiver end, the M spatial mode signals are demodulated by mixing with the LO in M optical front ends, which are composed of 90-degree hybrids, photodiodes and Trans-impedance amplifiers. The finite linewidth of both transmitter and LO will induce the phase noise to demodulated signals, which has to be estimated. The ADC is used to re-sample the analog signals at Nyquist sampling rate. In DSP, CD and DMGD can be compensated with frequency domain equalizers, phase noise can be estimated various phase estimation methods, and bit-error rate (BER) is finally estimated.

4.2 FMF system model and impairments

The FMF transmission link can be described by the following model:

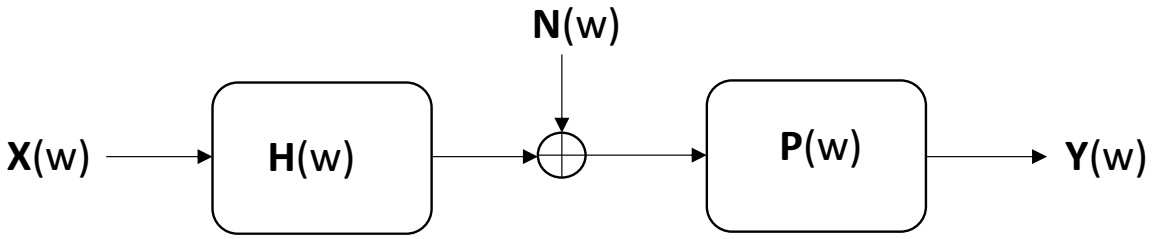

Figure 7. FMF transmission link model

where $\mathbf{Y}(w)$ is frequency domain output signals vector $[\mathbf{Y}_1(w), \mathbf{Y}_2(w), \ldots \mathbf{Y}_M(w)]^T$, M is number of modes in FMF systems, and w is angular frequency. $\mathbf{Y}_M(w)$ represents the frequency domain output signal on mode #M. $\mathbf{X}(w)$ is the frequency domain M input signals

vector $[\mathbf{X}_1(w), \mathbf{X}_2(w), \ldots \mathbf{X}_M(w)]^T$, and $\mathbf{X}_M(w)$ represents the frequency domain of input signal on mode #M. From the figure, the output $\mathbf{Y}(w)$ can be derived as follows:

$$\mathbf{Y}(w)= (\mathbf{H}(w)\cdot \mathbf{X}(w)+ \mathbf{N}(w))\cdot \mathbf{P}(w) \tag{4.1}$$

$\mathbf{H}(w)$ is the frequency domain representation of transmission matrix. For M-mode FMF transmission system, the $\mathbf{H}(w)$ is as follows:

$$\mathbf{H}(w)= \begin{pmatrix} \mathbf{H}_{11}(w) & \mathbf{H}_{12}(w) & \cdots & \mathbf{H}_{1M}(w) \\ \mathbf{H}_{21}(w) & \mathbf{H}_{22}(w) & \cdots & \mathbf{H}_{2M}(w) \\ \vdots & \vdots & & \vdots \\ \mathbf{H}_{M1}(w) & \mathbf{H}_{M2}(w) & \cdots & \mathbf{H}_{MM}(w) \end{pmatrix}$$

where $\mathbf{H}_{ij}(w)$ is the frequency domain impulse response, which characterizes the mode coupling effect of mode #j signal on mode #i signal. This individual frequency domain impulse response is determined by the link distortion, including CD, DMGD, MDL/MDG, and so on.

$\mathbf{N}(w)$ is the frequency domain representation of ASE noise, which is induced by optical amplifiers in transmission link. The ASE noise is more like white Gaussian noise with flat power spectrum density. In the long haul system, because many optical amplifiers are used in the transmission link, the ASE noise mainly determines the system performance. $\mathbf{P}(w)$ is the frequency domain passband filter, which is used to suppress the out of band ASE added on the signal power spectrum. The bandwidth of $\mathbf{P}(w)$ should be equal or slightly larger than modulated signal bandwidth, in order to ensure no ISI is induced by narrow filtering.

4.2.1 Chromatic dispersion

The fiber chromatic dispersion is resulted from the intrinsic wavelength independent refractive index of used fiber. The CD induces the different transmission delay for the

frequency components of modulated signals. The frequency domain expression of CD is as follows:

$$\mathbf{H}_{CD}(w)=\exp(-j/2\cdot\beta_2\cdot L_{fiber}\, w^2) \tag{4.2}$$

where β_2 is fiber group velocity dispersion, which is usually equal to 20 ps/nm/km. L_{fiber} is the transmission link length.

In amplitude modulated systems, the CD results in the signal pulse spreading, which make the direct detector hard to differentiate 0 or 1 bits. In phase modulated systems, the CD additionally results in the phase change of each symbol. In current systems, the link CD needs to be estimated first, and a fixed frequency domain equalizer, which has inverse equalization matrix of the CD, is used for its compensation.

4.2.2 Differential mode group delay

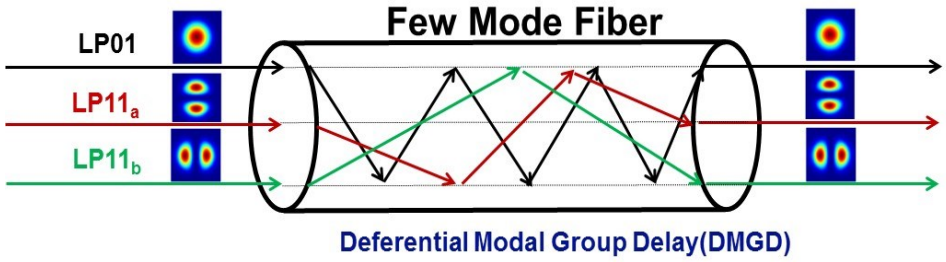

Figure 8. Concept of DMGD in few-mode fibers

Figure 8 shows the concept of DMGD in a 3-mode FMF. The three modes are LP_{01}, LP_{11a}, and LP_{11b}. Because of the mode dependent refractive index, 3 spatial modes have different transmission delay. Also, because all spatial modes are transmitted in the same physical area, there is inevitable inter-modal crosstalk. When the power of symbols is transferred from one mode to another mode until detection, it causes inter-modal crosstalk.

When the power of the symbol is transferred from one mode to another and transferred back, it causes ISI on that spatial channel. The inter-modal crosstalk and DMGD of a short length M-mode FMF can be described by the matrix $\mathbf{H}_{DMGD}$ in Figure 9.

$$\mathbf{H}_{DMGD}(w)=\begin{pmatrix} \mathbf{C}_{11} & \cdots & \mathbf{C}_{12} & \cdots & \mathbf{C}_{1M} \\ \mathbf{C}_{21} & \cdots & \mathbf{C}_{22} & \cdots & \mathbf{C}_{2M} \\ \vdots & & \vdots & & \vdots \\ \mathbf{C}_{M1} & & \mathbf{C}_{M2} & \cdots & \mathbf{C}_{MM} \end{pmatrix} \begin{pmatrix} \exp(-jw\tau_1) & \cdots & 0 \\ 0 & \exp(-jw\tau_2) & \cdots & 0 \\ \vdots & \vdots & \vdots & \vdots \\ 0 & 0 & \cdots & \exp(-jw\tau_M) \end{pmatrix}$$

Figure 9. Transfer function of DMGD and mode coupling of a short length FMF.

where τ_i is the propagation delay on mode #i, and C_{ij} is the coupling coefficient between mode #i and mode #j.

The transfer function of DMGD and mode coupling of a long FMF can be described by the concatenation of multiple short length transfer functions as follows:

$$\mathbf{H}_{DMGD,\,total}(w)= \mathbf{H}_{DMGD,\,1}(w)\cdot \mathbf{H}_{DMGD,\,2}(w)\cdots \mathbf{H}_{DMGD,\,N}(w) \qquad (4.3)$$

In FMF systems, the adaptive MIMO equalizer is used to compensate the DMGD and random mode coupling.

4.2.3 ASE noise

Figure 10. (Left) Signal constellation without ASE. (Right) Signal constellation with ASE

The ASE noise comes from optical amplifiers in the transmission link. It can be modeled as white Gaussian noise, which has the flat power spectral density. In optical systems, optical signal to noise ratio is used to evaluate the relative intensity of ASE noise power over optical signal power. The ASE noise induces the scattered signal constellation, as shown in Figure 10 [29].

4.2.4 Phase noise

In optical communication systems, the finite linewidth of both transmitter laser and local oscillator can bring up the phase noise into optical signals. As described in [30], the phase noise can be considered as a wiener process as follows:

$$\theta(k)= \theta(k-1)+\upsilon(k) \tag{4.4}$$

where $\theta(k)$ is the phase noise term on the k^{th} symbol. $\upsilon(k)$ is a zero-mean white Gaussian variable. Its variance is:

$$\sigma(k)=2\pi\cdot(\Delta\nu_{TX}+ \Delta\nu_{LO})\cdot T \tag{4.5}$$

where $\Delta\nu_{TX}$ and $\Delta\nu_{LO}$ are the transmitter and LO laser linewidth. T is the symbol interval.

Since phase noise adds random phase shift to the phase modulated signal, the signal constellation will be scattered to form a ring, as shown in Figure 11 [29].

Figure 11. (Left) constellation without phase noise. (Right) Constellation with phase noise

4.3 Coherent detection with DSP

In FMF transmission systems, coherent detection is used to demodulate spatial modes signals after transmission, and DSP will electrically compensate the CD, DMGD and phase noise. The architecture of coherent detection together with DSP for M-mode FMF transmission is shown in Figure 12.

It can be seen that M modes transmission requires M coherent receivers. In the coherent receiver, each spatial mode signal is demodulated into I and Q components by beating with LO in 90 degree hybrid, as shown in the following equation (Mode #1 as an example):

$$E_{i1,1}(t) = \frac{1}{2}(E_1(t) + E_{LO}(t)) \tag{4.6}$$

$$E_{i1,2}(t) = \frac{1}{2}(E_1(t) - E_{LO}(t)) \tag{4.7}$$

$$E_{q1,1}(t) = \frac{1}{2}(E_1(t) + jE_{LO}(t)) \tag{4.8}$$

$$E_{q1,2}(t) = \frac{1}{2}(E_1(t) - jE_{LO}(t)) \tag{4.9}$$

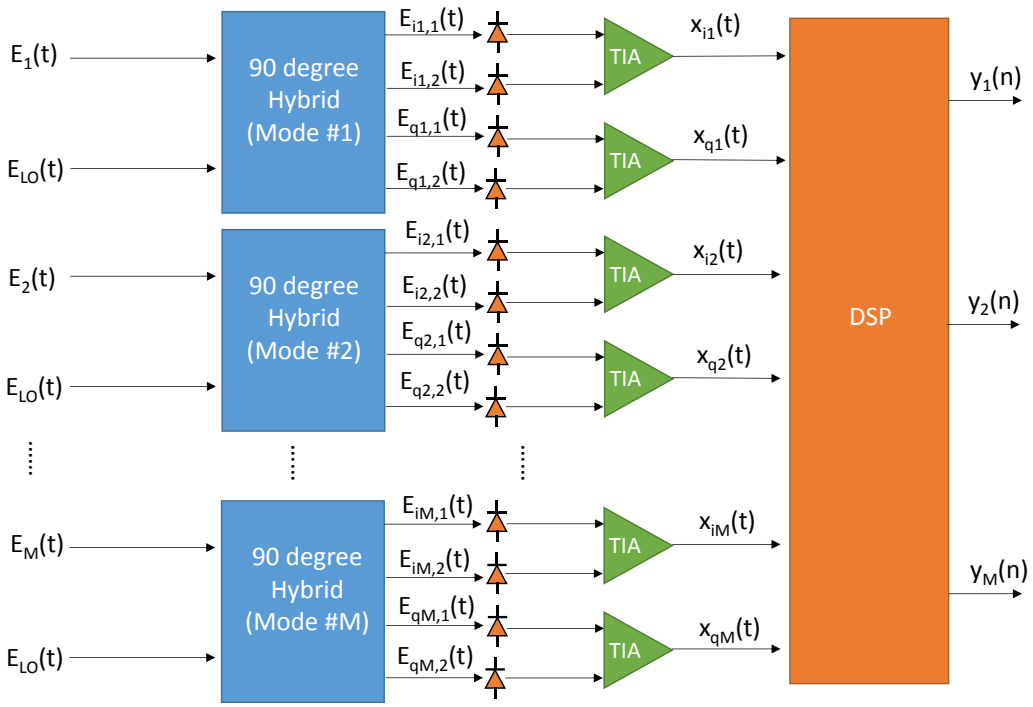

Figure 12. Coherent detection with DSP for M-mode FMF transmission

CHAPTER 5: MIMO DIGITAL SIGNAL PROCESING IN FMF SYSTEMS

5.1 Adaptive MIMO equalizer for DMGD compensation

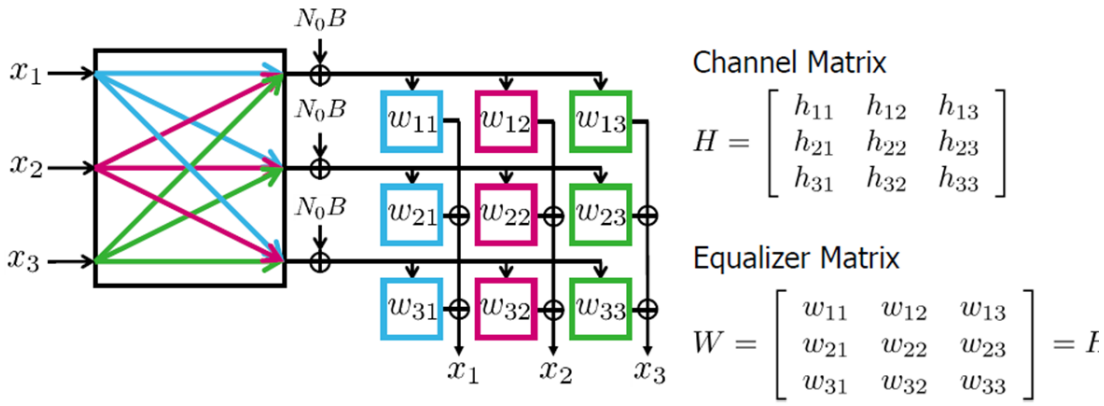

Figure 13. Architecture of the MIMO equalizer in 3-mode FMF systems

It has been extensively proposed that adaptive MIMO equalizer can effectively compensate the large DMGD and random inter-modal crosstalk, thus de-multiplexing the signals on different spatial modes. Figure 13 shows the MIMO equalizer architecture for 3-mode FMF systems as an example [31].In M-mode FMF systems, M^2 SISO equalizers are required to build up a M×M MIMO equalizer, in which the required tap length or hardware complexity of every SISO equalizer is linearly dependent on the accumulated DMGD. To completely compensate the signal distortion, the MIMO equalizer matrix **W** should be ideally inverse to the channel matrix **H**. The MIMO equalizer can be implemented either in the time domain or in the frequency domain. However, many research articles have demonstrated that the frequency domain approach can achieve much lower hardware complexity than time domain approach while keeping the same equalization performance. Since the fiber channel is dynamically changing, certain length training sequences need to be

periodically sent during system operation in order to accurately estimate the channel matrix. The length of training sequence is determined by the convergent rate of the MIMO equalizer. If the equalizer converges faster, fewer symbols in the training sequence are needed. However, if the equalizer converges slower, more symbols in the training sequence are required, which will decrease the overall system efficiency.

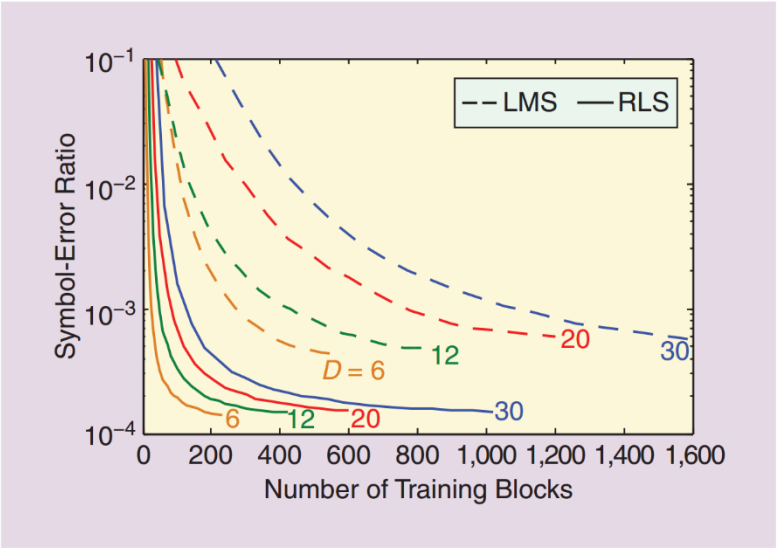

Figure 14. Convergent rate comparison of LMS and RLS algorithms

Two adaptive MIMO equalization methods have been proposed for DMGD compensation in FMF systems. One is the recursive least square (RLS) method, which has a fast convergent rate by paying extremely high hardware complexity. The other method is the least mean square (LMS) approach, which is widely used in FMF systems, for it is a good compromise among convergence rate, hardware complexity, and equalization performance. The comparison between LMS and RLS in terms of complexity and convergence rate is shown in Figure 14 and Figure 15 [32]. As shown in Figures 14 and 15, to achieve the stable

symbol error ratio of 1e-3 in a 6-mode transmission system, the RLS algorithm only needs ten times less training symbols than LMS algorithm by paying two times more hardware complexity. Compared with RLS algorithm, the frequency domain least mean square algorithm has much lower complexity. Especially for the long-haul transmission systems where the accumulated DMGD is pretty larger, the FD-LMS method can save much more hardware complexity than RLS algorithm.

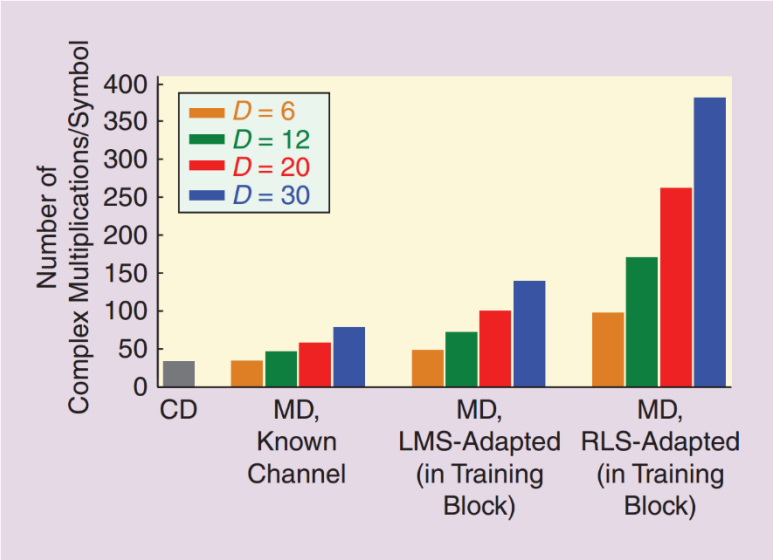

Figure 15. Hardware complexity comparison of RLS and LMS algorithms

5.2 Time-domain least mean square algorithm based adaptive MIMO equalizer

Figure 16 shows the architecture of adaptive TD-LMS equalization for mode #1 in an M-mode FMF system. Note that the equalizers for other M-1 output modes have the same architecture. After coherent detection and ADC re-sampling, each digital sequences $\mathbf{x}_1(n)$,

$\mathbf{x}_2(n)$, … $\mathbf{x}_M(n)$ is sent to the equalizer for the adaptive DMGD compensation. The equalization of k^{th} sample on mode #i is shown in (4.1).

$$y_i(k) = \sum_{j=1}^{M} \sum_{i=0}^{N} h_{ij}(i)\, x_j(k-i)) \tag{4.1}$$

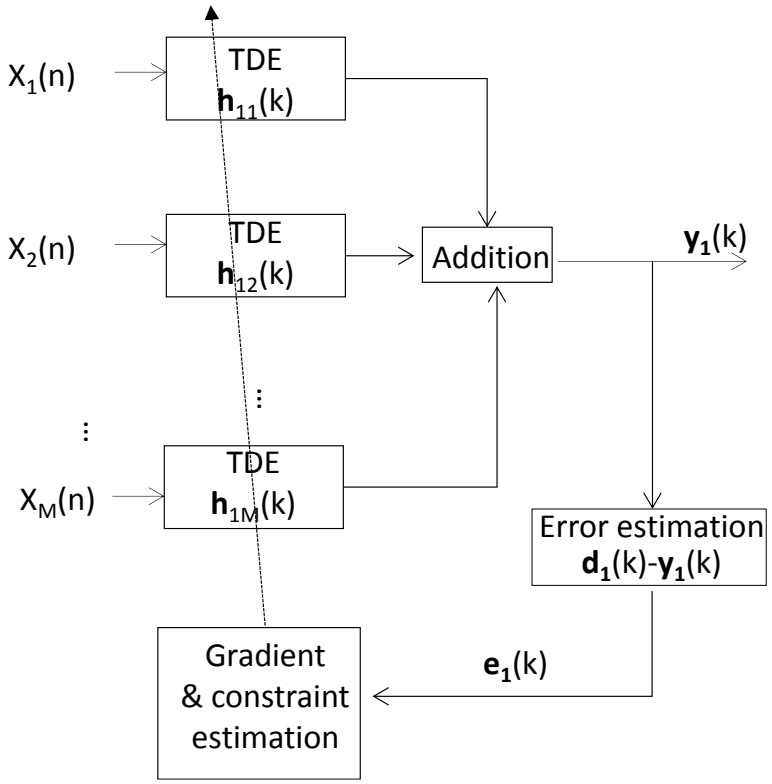

Figure 16. Architecture of adaptive TD-LMS equalizer for mode #1

where N is the number of filter taps, and i and j are mode index(1,2,3…M). Since there are two samples for each symbol after ADC, only one sample is saved as for each output symbol after equalization.

After equalization, every output sample is compared with the desired output, and the error result is fed into gradient and constraint estimation processing to update the equalizer tap coefficients, as shown in (4.2) and (4.3).

$$e_i(k) = d_i(k) - y_i(k) \tag{4.2}$$

$$\mathbf{h}_{ij} = \mathbf{h}_{ij} + \mu \cdot e_i(k) \cdot \mathrm{conj}(\mathbf{x}_j(k)) \tag{4.3}$$

where the μ is step size, which controls the convergence speed and equalization performance of the adaptive TD-LMS algorithm.

5.3 Frequency-domain least mean square algorithm based adaptive MIMO equalizer

Figure 17 shows the architecture of adaptive FD-LMS equalizer for mode #1 in an M-mode FMF system. Note that the equalizers for other M-1 modes have the same architecture. After coherent detection and ADC resampling, serial to parallel (S/P) converters divide each data sequence $\mathbf{x}_1(n)$, $\mathbf{x}_2(n)$, … $\mathbf{x}_M(n)$ into even and odd sequences $\mathbf{x}_1^e(n)$, $\mathbf{x}_1^o(n)$, $\mathbf{x}_2^e(n)$,$\mathbf{x}_2^o(n)$… $\mathbf{x}_M^e(n)$,$\mathbf{x}_M^o(n)$. The sequence $\mathbf{x}_j^p(n)$ is further divided into sequential block $\mathbf{x}_j^p(k)$ with N samples length. j is mode index (1, 2, …M), and p indicates even or odd sequence. Suppose that 50% overlap length in overlap-save method is used, N/2 samples of k^{th} block is overlapped with $(k-1)^{th}$ block. FFT transform matrix then convert each block $\mathbf{x}_j^p(k)$ to the frequency domain $\mathbf{X}_j^p(k)$ as shown in (4.4).

$$\mathbf{X}_j^p(k) = \mathrm{diag}\{\mathbf{F}[\mathbf{x}_j^p(k)]\} \tag{4.4}$$

where diag[] is the diagonal matrix operator, and **F** denotes a discrete Fourier transform (DFT) matrix. $\mathbf{X}_j^p(k)$ is a NxN matrix with its diagonal elements equivalent to the frequency bins of input block $\mathbf{x}_j^p(k)$.

Frequency domain equalization is realized by the multiplication between $\mathbf{X}_j^p(k)$ and corresponding equalizer $\mathbf{H}_{i,j}^p(k)$ and the additions of the multiplication results as shown in (4.5). i and j are both mode index (1, 2, …M). $\mathbf{H}_{i,j}^p(k)$ is an Nx1 vector, with its elements equivalent to the coefficients of the equalizer for output mode i with input mode j.

$$\mathbf{Y}_i(k) = \sum_{j=1}^{M} (\mathbf{X}_j^{\,e}(k) \cdot \mathbf{H}_{i,j}^{\,e}(k) + \mathbf{X}_j^{\,o}(k) \cdot \mathbf{H}_{i,j}^{\,o}(k)) \tag{4.5}$$

$$\mathbf{y}_i(k) = \mathbf{K}\mathbf{F}^{-1}\mathbf{Y}_i(k) \tag{4.6}$$

$$\mathbf{e}_i(k) = \mathbf{d}_i(k) - \mathbf{y}_i(k) \tag{4.7}$$

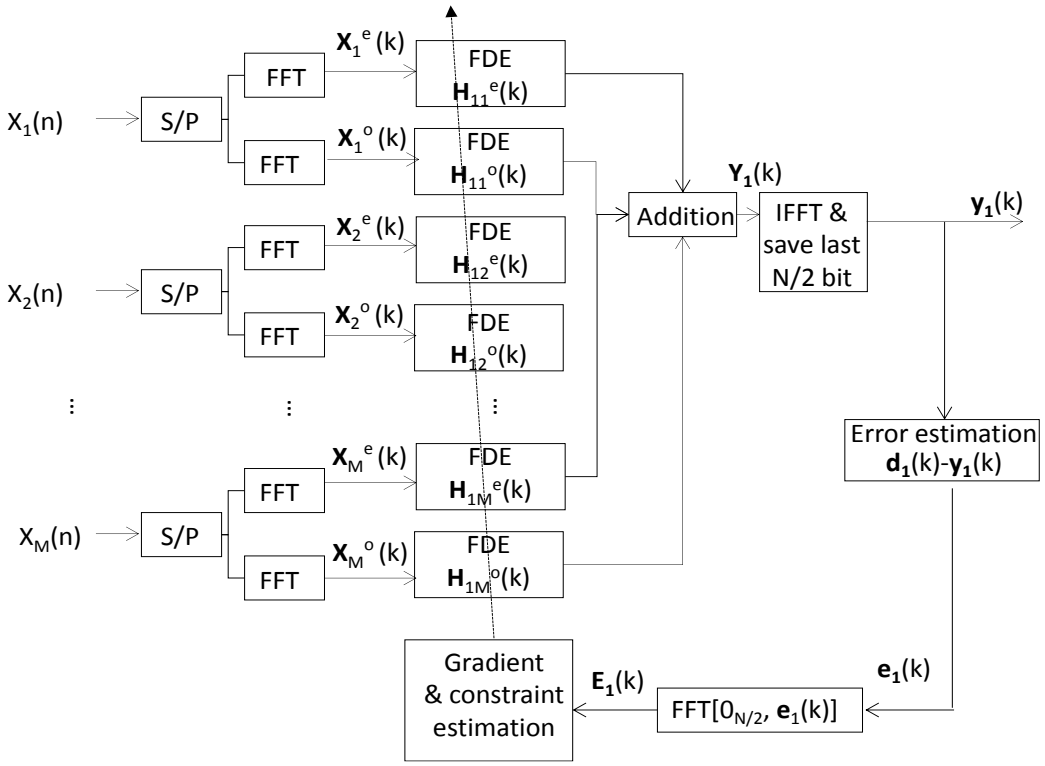

Figure 17. Concept of adaptive FD-LMS equalizer for mode #1 in FMF systems

After equalization, block $\mathbf{Y}_i(k)$ is converted to time domain block $\mathbf{y}_i(k)$ as shown in (4.6). $\mathbf{F}^{-1}$ is the inverse DFT (IDFT) matrix, and $\mathbf{K}$ is a constraint matrix $[\mathbf{0}_{N/2}\ \mathbf{I}_{N/2}]$. In the time domain block, only the last N/2 samples are saved.

The output block $\mathbf{y}_i(k)$ is used for posterior error estimation in feedback loop, as shown in (4.7), where $\mathbf{d}_i(k)$ is the desired output of k^{th} block on mode i.

In the gradient constraint and estimation algorithm, time domain posterior error block

$\mathbf{e}_i(k)$ is firstly prefixed with N/2 zeros and is converted to the frequency domain $\mathbf{E}_i(k)$ for updating the FDE as shown in (4.8) and (4.9).

$$\mathbf{E}_i(k) = \mathbf{F}\mathbf{K}^{\mathbf{T}}\mathbf{e}_i(k) \tag{4.8}$$

$$\mathbf{H}_{i,j}{}^{p}(k+1) = \mathbf{H}_{i,j}{}^{p}(k) + 2\mathbf{F}\mathbf{G}\mathbf{F}^{-1} \cdot \mathbf{U}_{ij}^{p}(k) \cdot [\mathbf{X}_j{}^{p}(k)]^{\mathbf{T}} \cdot \mathbf{E}_i(k) \tag{4.9}$$

$\mathbf{G}=\mathbf{I}_N-\mathbf{Q}$, and $\mathbf{Q}$ is a constraint matrix $[\mathbf{0}_{N/2}, \mathbf{0}_{N/2}, \mathbf{0}_{N/2}, \mathbf{I}_{N/2}]$. The matrix G and Q are used for saving only the first and last half of each block respectively. According to [33], $\mathbf{FGF}^{-1}$ and $\mathbf{FQF}^{-1}$ approximately equal to $1/2 \cdot \mathbf{I}_N$. $\mathbf{U}_{ij}{}^{p}(k)$ is the step size matrix for the equalizer $\mathbf{H}_{i,j}{}^{p}(k)$ and equals to diag$\{\mu_{ij,0}{}^{p}(k), \mu_{ij,1}{}^{p}(k),\ldots, \mu_{ij,N-1}{}^{p}(k)\}$. The step size is a key parameter in determining both equalization performance and convergence speed of the adaptive FD-LMS algorithm. In the conventional adaptive FD-LMS algorithm [18], all elements of $\mathbf{U}_{ij}{}^{p}(k)$ are set to the same value μ.

5.4 Comparison between adaptive TD-LMS and adaptive FD-LMS algorithms

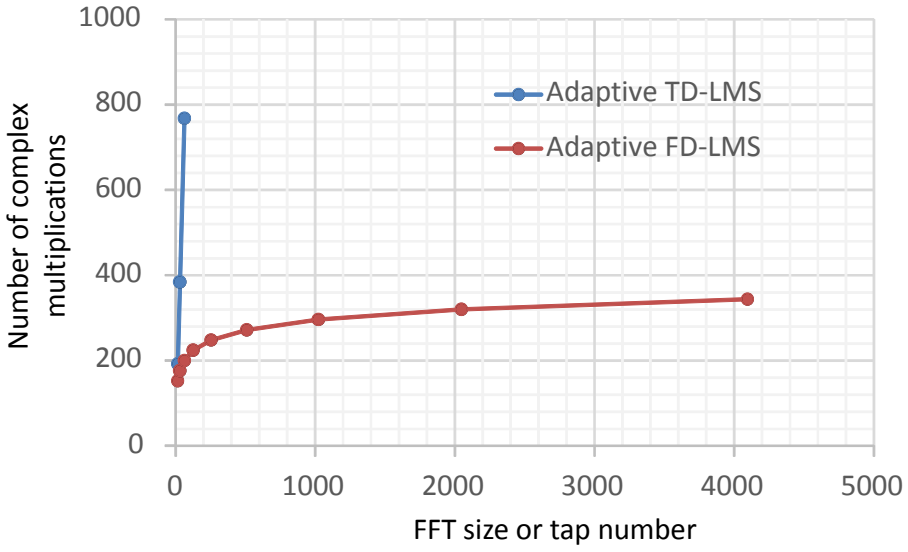

Figure 18. Hardware complexity comparison for DMGD compensation

Figure 18 shows the required complex multiplications at different required tap number or FFT size for DMGD compensation in a 2-mode system. It can be seen that when the tap number or FFT size is very small, the adaptive TD-LMS requires less complex multiplications than adaptive FD-LMS. However, adaptive FD-LMS requires much less complex multiplications than TD-LMS when the required tap number or FFT size is larger.

Figure 19 shows the DMGD compensation of both TD-LMS and FD-LMS. In the simulation, 2200 ps DMGD is induced and 256 taps TD-LMS and 256 FFT size FD-LMS methods are compared in compensating DMGD. It can be seen that both FD-LMS and TD-LMS with a sufficient number of taps (or FFT size) can completely compensate the channel induced DMGD.

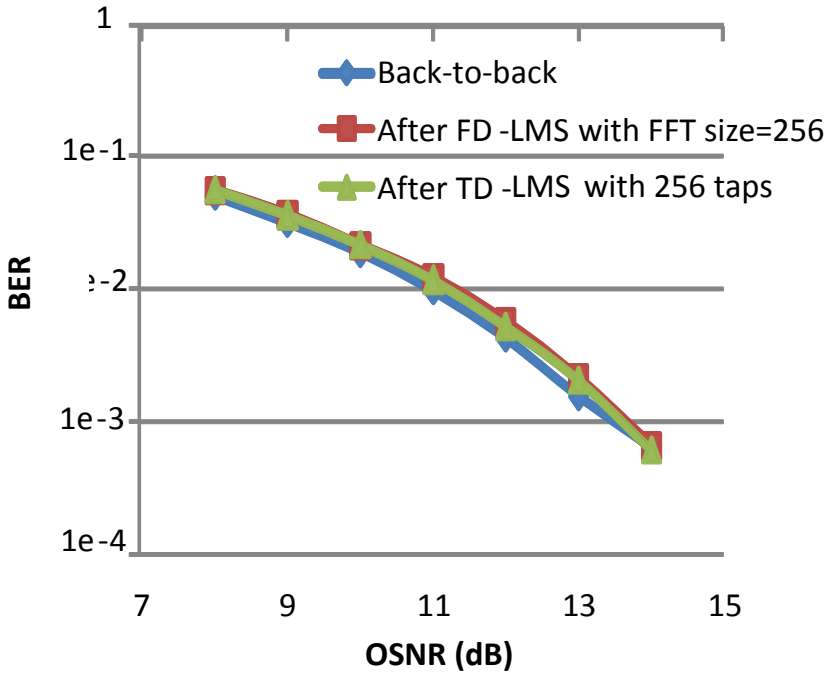

Figure 19: Performance comparison for DMGD compensation

CHAPTER 6: SINGLE-STAGE MIMO EQUALIZER IN FMF SYSTEMS

6.1 Principle of single-stage MIMO equalizer

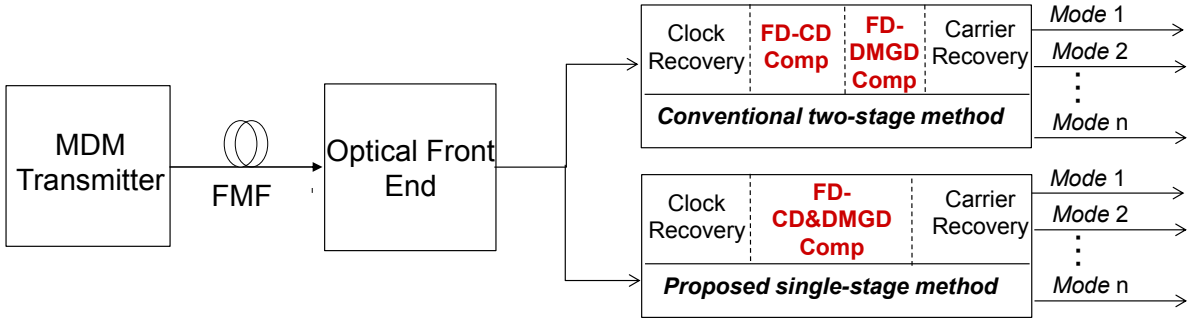

Figure 20. Comparison of proposed single-stage equalizer and conventional two-stage equalizer

In FMF transmission system, except for DMGD, CD is another linear distortion that needs to be compensated in DSP. In conventional single-mode fiber transmission systems, because CD is much larger than PMD, a separate CD compensation equalizer is needed before using an MIMO equalizer for PMD compensation. The same equalization architecture is simply immigrated to FMF transmission systems, in which a two-stage equalization method is used to compensate the CD by a static FDE in the first stage and compensate DMGD by adaptive FD-LMS in the second stage, as shown in Figure 20. However, because the accumulated DMGD is usually much larger than CD in FMF systems, which means the equalizer length of adaptive FD-LMS is greater than that of static FDE in FMF systems, such that the same adaptive FD-LMS equalizer used for DMGD compensation can also be used for CD compensation without increasing the adaptive equalizer length. Such a single-stage

equalizer can eliminate the need for an independent CD compensation module, thus can reduce hardware complexity of DSP in FMF transmission systems.

6.2 Single-stage MIMO equalizer architecture

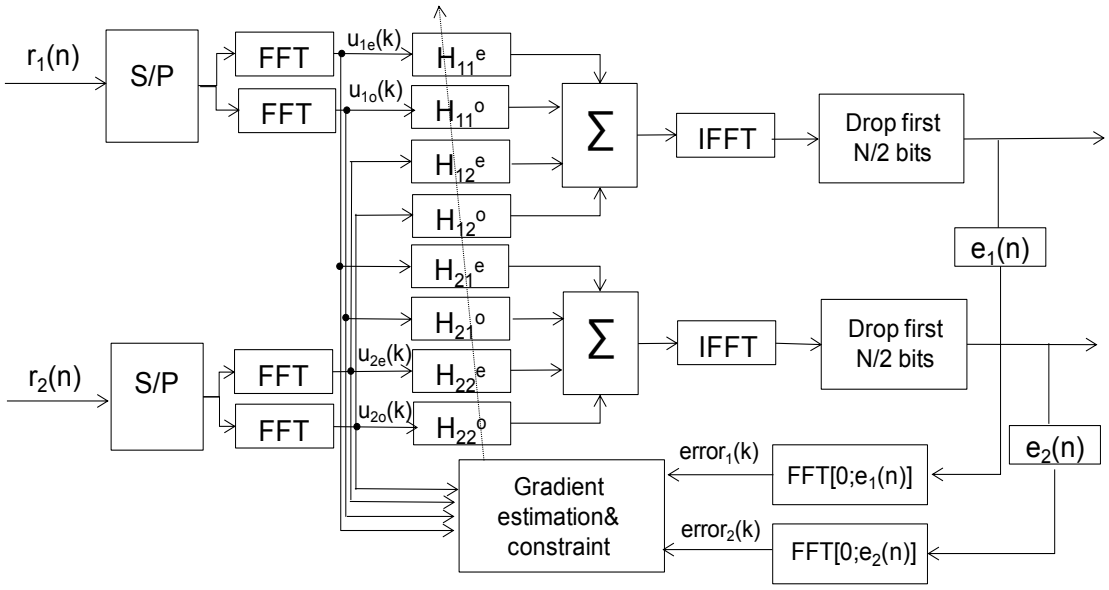

Figure 21. Architecture of the adaptive FD-LMS equalizer in 2-mode systems

Figure 21 shows the concept of adaptive MIMO equalizer for 2-mode FMF transmission systems, which is similar to Figure 17.

6.3 Simulation setup

An 112 Gbit/s two-mode transmission system is simulated as shown in Figure 22, where each mode carries a 56 Gbit/s QPSK signal. The FMF model in the simulation is similar to the one in [34]. In the simulation, DMGD is 0.076 ps/m between two modes, and CD and CD slope are 20 ps/nm·km and 0.065 ps/nm^2·km respectively [11]. 100 times mode couplings with -25 dB each is simulated. The optical noise is added after the FMF transmission and an optical filter is used to suppress the noise before coherent detection. The fiber loss is assumed to be

completely compensated by the FMF EDFA, and therefore is not included in this simulation. Before MIMO processing, the two electrical signals are re-sampled at two samples per symbol. We also compare the performance and complexity of our proposed method with the conventional two-stage method, in which the first stage is a static frequency-domain CD compensator and the second stage is the FD-LMS MIMO equalizer. After MIMO processing, the BER and Q value are estimated for each mode.

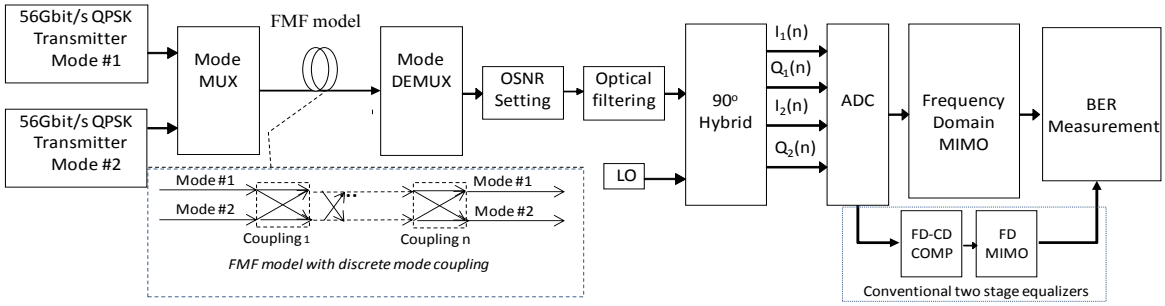

Figure 22. Simulation setup for the 112 Gbit/s two-mode coherent transmission system

6.4 Simulation results

Figure 23 shows the equalization results of both single-stage method and two-stage methods. It can be seen that the proposed single-stage method can completely compensate the fiber induced CD and DMGD simultaneously at both 1000 km and 420 km transmission.

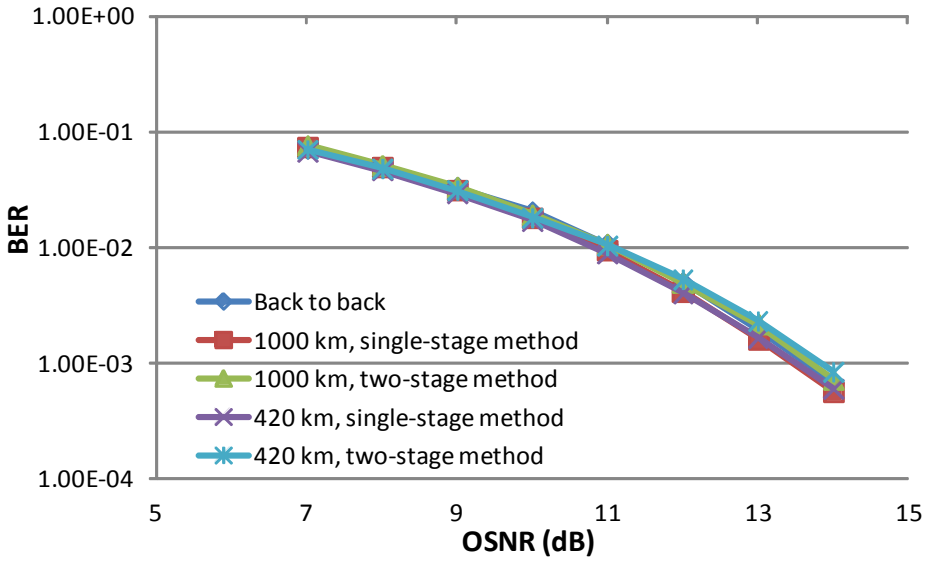

Figure 23. Compensation performance comparison between single-stage method and two-stage method at difference transmission distances.

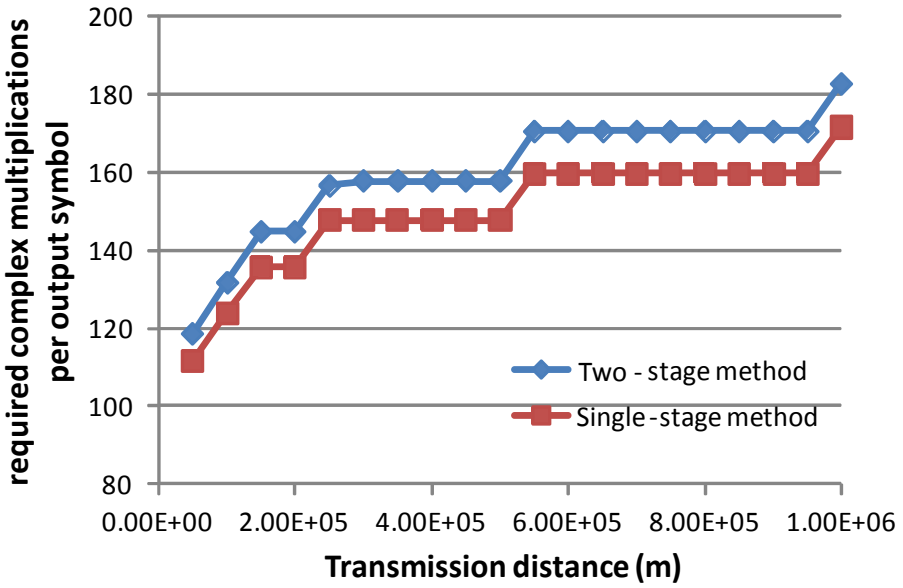

Figure 24. Required complex multiplications per output symbol of single-stage and two-stage methods at different transmission distance

Figure 24 shows the required complex multiplications per output symbol of single-stage method and two-stage method at different transmission distance. At the same transmission distance, both methods use the same FFT size for DMGD compensation, while the FFT size of

static FDE in two-stage method is determined by the fiber induced CD. Note that, due to the fast computation speed of the classic radix-2 FFT algorithm, which requires $N \cdot \log_2(N)/2$ complex multiplications for N points FFT [35], 2^n FFT size is used for both static FDE in first stage of single-stage method and adaptive FD-LMS of both two methods. Suppose N_{DMGD} FFT size is needed for DMGD compensation, adaptive FD-LMS algorithm consumes $12\log_2 N_{DMGD}$ +32 per output symbol after equalization. If the compensating fiber induced CD requires N_{CD} FFT size in first stage FDE, the two-stage method needs consume additional $\log_2 N_{CD}$ +2 complex multiplication per output symbol. Figure 4 shows that, for transmission distance from 50km up to 1000km, the single-stage method always consumes less complex multiplications than the conventional two-stage method. For example, to compensate 1000 km and 420 km induced CD and DMGD, both single-stage and two-stage methods need 8192, 2048 FFT size in adaptive FD-LMS algorithm respectively, while the two-stage method also need additional 512, 256 FFT size in the first-stage static FDE for CD compensation. So, the two-stage method consumes 199 and 174 complex multiplications per output symbol at 1000km and 420km transmission, while the proposed single-stage method consumes only 188 and 164 complex multiplications per output symbol at the same transmission distance.

Figure 25 shows the step size of adaptive FD-LMS algorithm in single-stage and two-stage methods versus transmission distance. The OSNR is set to 14 dB. For 1000 km and 720 km transmission, 8192 and 4096 FFT size are used in adaptive FD-LMS respectively, and 512 FFT size is used for the first-stage FDE of the two-stage method. Figure 25 shows that, for the same transmission distance, the maximum step sizes to achieve the same Q value after equalization are identical for both methods. To achieve <0.3dB Q-penalty in 1000 km and 720 km transmission, the maximum step sizes are $1.5e^{-5}$ and $3e^{-5}$, respectively.

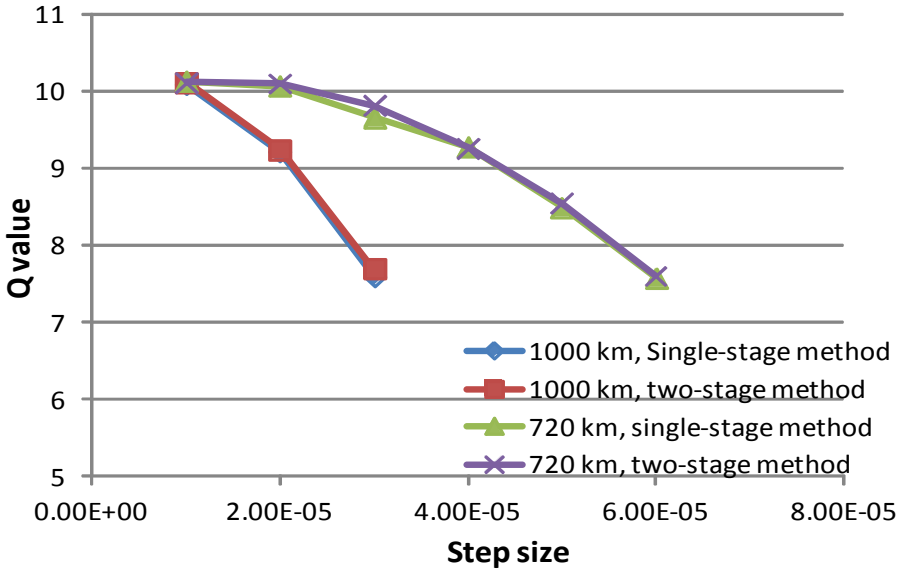

Figure 25. Step size of adaptive FD-LMS vs Q value after equalization using both single-stage method and two-stage method in two different distance

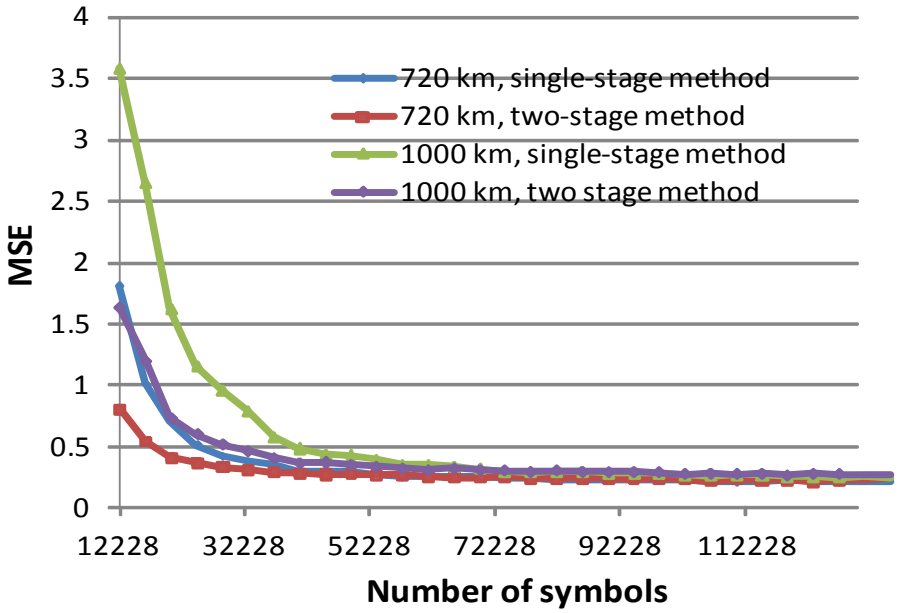

Figure 26. Required number of blocks for convergence of adaptive FD-LMS in both single-stage and two-stage methods for 1000 km transmission

Figure 26 shows the required number of blocks for convergence of FD-LMS in both single-stage and two-stage methods to achieve <0.3 dB Q-penalty. The step sizes are $1.5e^{-5}$ and $3e^{-5}$ for 1000 km and 720 km transmission, respectively. It can be seen that the mean square error (MSE) of the proposed single-stage method is larger than two-stage method at the initial convergence. The reason for this is that the prior FDE CD compensation of two-stage method decreases the initial MSE. So, the single-stage method may have less convergence speed than the conventional two-stage method. However, if we set the initial frequency response of adaptive FD-LMS to already known frequency response of channel CD, the single-stage method can probably achieve the same convergence speed as the two-stage method. Furthermore, our single-stage adaptive equalization method eliminates the need for CD estimation that is required for conventional two-stage method, i.e. our method allows automatic CD compensation without any knowledge about the actual CD values. This could be a significant advantage for a dynamic optical network where the optical link length and therefore CD does not remain a constant.

CHAPTER 7: FAST CONVERGENT FREQUENCY-DOMAIN LEAST MEAN SQUARE ALGORITHMS

7.1 Fast convergent step size control methods

Figure 27 shows the architecture of the fast convergent adaptive FD-LMS algorithm with phase estimation in an M-mode FMF systems. As shown in Figure 27, after coherent detection, the analog signals on different spatial modes are firstly re-sampled at two samples

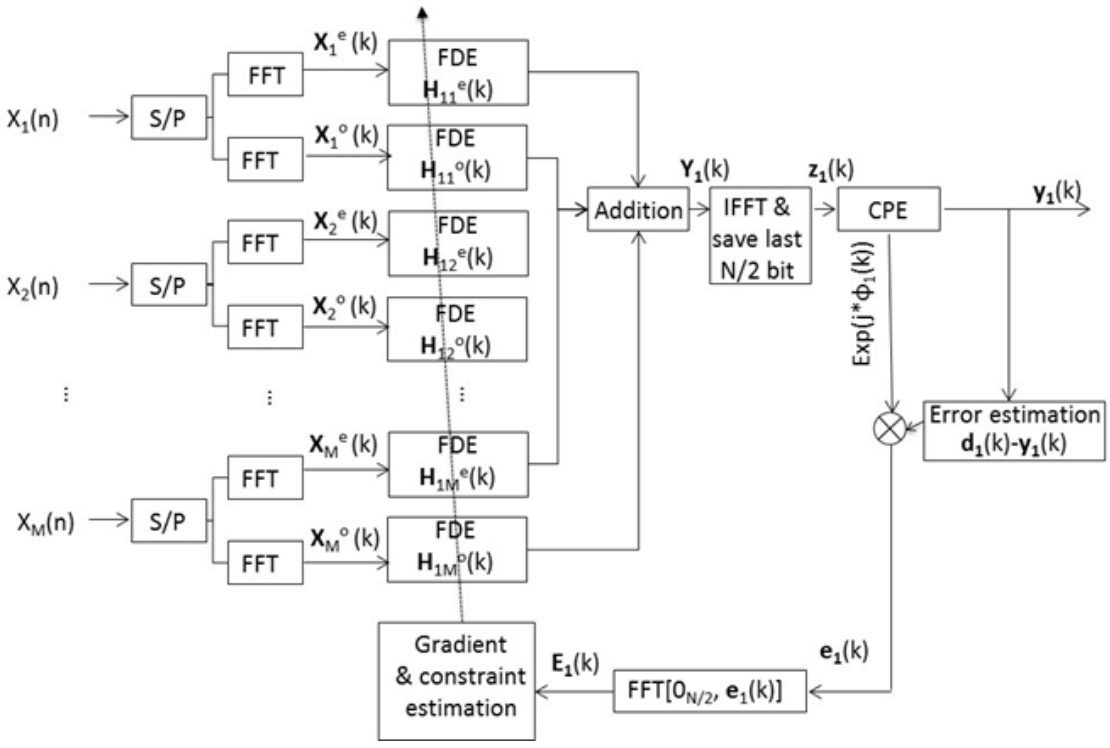

Figure 27 Architecture of M×M adaptive FD-LMS equalizer with phase estimation

per symbol. S/P converters then divide each data sequence $\mathbf{x}_1(n)$, $\mathbf{x}_2(n)$, $\cdots$ $\mathbf{x}_M(n)$ into even and odd sequences $\mathbf{x}_1^e(n)$, $\mathbf{x}_1^o(n)$, $\mathbf{x}_2^e(n)$,$\mathbf{x}_2^o(n)$,$\cdots$ $\mathbf{x}_M^e(n)$,$\mathbf{x}_M^o(n)$. The sequence $\mathbf{x}_j^p(n)$ is further divided into sequential block $\mathbf{x}_j^p(k)$, where N/2 samples of the k^{th} block are overlapped with the $(k-1)^{th}$ block. Here, j is mode index (1, 2,$\cdots$M), and p indicates even or

odd sequence. Each block $\mathbf{x}_j^p(k)$ is then converted to frequency domain $\mathbf{X}_j^p(k)$ with FFT as shown in (7.1).

$$\mathbf{X}_j^p(k) = \mathrm{diag}\{\mathbf{F}[\mathbf{x}_j^p(k)]\} \tag{7.1}$$

where diag{} is the diagonal matrix operator, and $\mathbf{F}$ denotes a DFT matrix. $\mathbf{X}_j^p(k)$ is an N×N matrix with its diagonal elements equivalent to the frequency bins of input block $\mathbf{x}_j^p(k)$.

As shown in (7.2), frequency domain equalization is realized by the multiplication between $\mathbf{X}_j^p(k)$ and the corresponding equalizer $\mathbf{H}_{i,j}{}^p(k)$, and then the additions of the multiplication results. Here, i and j are both mode indices (1, 2,···M).

$$\mathbf{Y}_i(k) = \sum_{j=1}^{M}(\mathbf{X}_j{}^e(k) \cdot \mathbf{H}_{i,j}{}^e(k) + \mathbf{X}_j{}^o(k) \cdot \mathbf{H}_{i,j}{}^o(k)) \tag{7.2}$$

After equalization, block $\mathbf{Y}_i(k)$ on mode i is converted to time domain block $\mathbf{z}_i(k)$ as shown in (7.3), which is used for the next stage M[th] carrier phase estimation (CPE) [13]. Here, $\mathbf{F^{-1}}$ is the inverse IDFT matrix, and $\mathbf{K}$ is a constraint matrix $[\mathbf{0}_{N/2}\ \mathbf{I}_{N/2}]$.

As shown in (7.4), the equalizer's final output block $\mathbf{y}_i(k)$ is used for the prior error estimation in the feedback loop, where $\mathbf{d}_i(k)$ is the desired output of the k[th] block on mode i, and $\boldsymbol{\varphi}_i(k)$ is the estimated phase noise of block $\mathbf{z}_i(k)$.

$$\mathbf{z}_i(k) = \mathbf{K}\mathbf{F^{-1}}\mathbf{Y}_i(k) \tag{7.3}$$

$$\mathbf{e}_i(k) = (\mathbf{d}_i(k) - \mathbf{y}_i(k)) \cdot \exp(j \cdot \boldsymbol{\varphi}_i(k)) \tag{7.4}$$

In the gradient and constraint estimation, the time domain prior error block $\mathbf{e}_i(k)$ is firstly prefixed with N/2 zeros and converted to the frequency domain $\mathbf{E}_i(k)$ for updating the FDE, as shown in (7.5) and (7.6).

$$\mathbf{E}_i(k) = \mathbf{F}\mathbf{K}^\mathbf{T}\mathbf{e}_i(k) = \{\mathbf{F}\mathbf{K}^\mathbf{T}\mathbf{d}_i(k) - \mathbf{F}\mathbf{Q}\mathbf{F^{-1}}[\sum_{j=1}^{M}(\mathbf{X}_j{}^e(k) \cdot \mathbf{H}_{i,j}{}^e(k) + \mathbf{X}_j{}^o(k) \cdot \mathbf{H}_{i,j}{}^o(k))]\}\exp(j \cdot \boldsymbol{\varphi}_i(k)) \tag{7.5}$$

$$\mathbf{H}_{i,j}{}^{p}(k+1) = \mathbf{H}_{i,j}{}^{p}(k) + 2\mathbf{FGF^{-1}} \cdot \mathbf{U}_{ij}^{p}(k) \cdot [\mathbf{X}_j{}^{p}(k)]^{\mathbf{T}} \cdot \mathbf{E}_i(k) \quad (7.6)$$

Here, $\mathbf{G}=\mathbf{I}_N-\mathbf{Q}$, and $\mathbf{Q}$ is a constraint matrix $[\mathbf{0}_{N/2}, \mathbf{0}_{N/2;}\mathbf{0}_{N/2,}\mathbf{I}_{N/2}]$. The matrices Q and G are used for saving the first and the second half of each block, respectively. $\mathbf{FGF^{-1}}$ and $\mathbf{FQF^{-1}}$ approximately equal $1/2\cdot\mathbf{I}_N$, and $\mathbf{U}_{ij}{}^{p}(k)$ is the step size matrix for the equalizer $\mathbf{H}_{i,j}{}^{p}(k)$ which equals to $\mathrm{diag}\{\mu_{ij,0}{}^{p}(k), \mu_{ij,1}{}^{p}(k),\ldots, \mu_{ij,N-1}{}^{p}(k)\}$. This step size matrix determines both equalization performance and convergence speed of the adaptive FD-LMS algorithm. In the conventional adaptive FD-LMS algorithm, all elements of $\mathbf{U}_{ij}{}^{p}(k)$ are set as the same value μ.

In [33], it is proposed that, in SISO systems, one way to find the optimal bin-wise step size for the adaptive FD-LMS algorithm is to cancel the posterior error of each frequency bin. In M×M MIMO systems, the posterior error of the k^{th} equalized block on mode i is defined in (7.7).

$$\mathbf{p}_i(k) = \mathbf{d}_i(k) - \mathbf{KF^{-1}} \cdot \{\textstyle\sum_{j=1}^{M}(\mathbf{X}_j{}^{e}(k) \cdot \mathbf{H}_{i,j}{}^{e}(k+1) + \mathbf{X}_j{}^{o}(k) \cdot \mathbf{H}_{i,j}{}^{o}(k+1))\} \quad (7.7)$$

By combining (7.6) and (7.7), we could derive that

$$\mathbf{p}_i(k) = \mathbf{d}_i(k) - \mathbf{KF^{-1}} \cdot \{\textstyle\sum_{j=1}^{M}(\mathbf{X}_j{}^{e}(k) \cdot (\mathbf{H}_{i,j}{}^{e}(k) + 2\mathbf{FG^{-1}F} \cdot \mathbf{U}_{ij}^{e}(k) \cdot [\mathbf{X}_j{}^{e}(k)]^{\mathbf{T}} \cdot$$
$$\mathbf{E}_i(k)) + \mathbf{X}_j{}^{o}(k)(\mathbf{H}_{i,j}{}^{o}(k) + 2\mathbf{FG^{-1}F} \cdot \mathbf{U}_{ij}^{o}(k) \cdot [\mathbf{X}_j{}^{o}(k)]^{\mathbf{T}} \cdot \mathbf{E}_i(k))\} \quad (7.8)$$

From above equation, we could further derive that

$$\mathbf{p}_i(k) = \mathbf{d}_i(k) - \mathbf{y}_i(k) - \mathbf{KF^{-1}} \cdot \{ 2\mathbf{FG^{-1}F} \cdot \mathbf{E}_i(k) \cdot \textstyle\sum_{j=1}^{M}\big(\mathbf{U}_{ij}^{e}(k) \cdot \mathbf{X}_j{}^{e}(k) \cdot [\mathbf{X}_j{}^{e}(k)]^{T} +$$
$$\mathbf{U}_{ij}^{o}(k) \cdot \mathbf{X}_j{}^{o}(k) \cdot [\mathbf{X}_j{}^{o}(k)]^{T}\big)\} \quad (7.9)$$

(7.9) can be further derived as:

$$\mathbf{p}_i(k) = \mathbf{e}_i(k) - \{ 2\mathbf{KF^{-1}FG^{-1}F} \cdot \mathbf{E}_i(k) \cdot \textstyle\sum_{j=1}^{M}\big(\mathbf{U}_{ij}^{e}(k) \cdot \mathbf{X}_j{}^{e}(k) \cdot [\mathbf{X}_j{}^{e}(k)]^{T} +$$
$$\mathbf{U}_{ij}^{o}(k) \cdot \mathbf{X}_j{}^{o}(k) \cdot [\mathbf{X}_j{}^{o}(k)]^{T}\big)\} \quad (7.10)$$

The frequency domain of posterior error $\mathbf{p}_i(k)$ is

$$\mathbf{P}_i(k) = \mathbf{F}\mathbf{K}^{\mathbf{T}}\mathbf{p}_i(k) \tag{7.11}$$

Then,

$$\mathbf{P}_i(k) = \mathbf{F}\mathbf{K}^{\mathbf{T}}\mathbf{e}_i(k) - \{\, 2\mathbf{F}\mathbf{K}^{\mathbf{T}}\mathbf{K}\mathbf{F}^{-\mathbf{1}}\mathbf{F}\mathbf{G}^{-\mathbf{1}}\mathbf{F}\cdot\mathbf{E}_i(k)\cdot$$

$$\sum_{\mathbf{j=1}}^{\mathbf{M}}\left(\mathbf{U}_{ij}^{e}(k)\cdot\mathbf{X}_j^{\,e}(k)\cdot[\mathbf{X}_j^{\,e}(k)]^T + \mathbf{U}_{ij}^{o}(k)\cdot\mathbf{X}_j^{\,o}(k)\cdot[\mathbf{X}_j^{\,o}(k)]^T\right)\} \tag{7.12}$$

Further, according to (7.5),

$$\mathbf{F}\mathbf{K}^{\mathbf{T}}\mathbf{K}\mathbf{F}^{-\mathbf{1}} = \mathbf{F}\mathbf{Q}^{-\mathbf{1}}\mathbf{F} \approx \frac{1}{2}\mathbf{I}_N \tag{7.13}$$

And

$$\mathbf{F}\mathbf{G}^{-\mathbf{1}}\mathbf{F} \approx \frac{1}{2}\mathbf{I}_N \tag{7.14}$$

The frequency domain representation of posterior error is:

$$\mathbf{P}_i(k) = \mathbf{E}_i(k)\{1 - \frac{1}{2}I_N\cdot\sum_{\mathbf{j=1}}^{\mathbf{M}}\left(\mathbf{U}_{ij}^{e}(k)\cdot\mathbf{X}_j^{\,e}(k)\cdot[\mathbf{X}_j^{\,e}(k)]^T + \mathbf{U}_{ij}^{o}(k)\cdot\mathbf{X}_j^{\,o}(k)\cdot[\mathbf{X}_j^{\,o}(k)]^T\right)\} \tag{7.15}$$

The m^{th} frequency bin of $\mathbf{P_i}(k)$ is:

$$\begin{aligned} P_{i,m}(k) = \{1 - \frac{1}{2}\sum_{j=1}^{M}(&\mu_{ij,m}^{e}(k)\,X_{j,m}^{e}(k)[X_{j,m}^{e}(k)]^H \\ &+\mu_{ij,m}^{o}(k)\,X_{j,m}^{o}(k)[X_{j,m}^{o}(k)]^H)\}\,E_{i,m}(k) \end{aligned} \tag{7.16}$$

After the convergence of the FDE, the DMGD induced distortion is completely compensated, and laser phase noise is effectively estimated by the CPE algorithm. The posterior error and prior error of each output block should both be equivalent to the background noise, as shown in (7.17).

$$S_{p,j,m}^{\,p}(k) = S_{e,j,m}^{\,p}(k) = S_{v,j,m}^{\,p}(k) \tag{7.17}$$

where $S_{p,j,m}^{\,p}(k)$ is the m^{th} bin of the PSD of posterior error block p (even/odd) on mode j; $S_{e,j,m}^{\,p}(k)$ is the m^{th} bin of the PSD of prior error block p on mode j; and $S_{v,j,m}^{\,p}(k)$ is the m^{th}

bin of the PSD of AWGN block p on mode j.

By taking the mean square of both sides of (7.16) and suppose that every input block is mutually independent, we can derive that:

$$S_{p,j,m}^{P}(k) = 1 - \sum_{i=1}^{M} \left(\frac{1}{2}\mu_{ji,m}^{e}(k) S_{x,i,m}^{e}(k) + \frac{1}{2}\mu_{ji,m}^{o}(k) S_{x,i,m}^{o}(k)\right) \cdot S_{e,i,m}(k) \qquad (7.18)$$

By combining (7.17) and (7.18), and considering that all the equalizers converge at the same rate, the step size $\mu_{ij,m}{}^{p}(k)$ can be derived as:

$$\mu_{ij,m}{}^{p}(k) = \frac{\alpha}{S_{x,j,m}{}^{p}(k)} \left(1 - \sqrt{\frac{S_{v,j,m}{}^{p}(k)}{S_{e,i,m}(k)}}\right) \qquad (7.19)$$

From (7.19), the controlled step size depends on the estimation of $s_{v,j,m}{}^{p}(k)$.

7.1.1 Signal PSD dependent FD-LMS algorithm

From (7.19), if the background noise is negligible, it can be simplified to (7.20). In (7.20), the step size control is only determined by the power of each frequency of the FFT block. For the frequency bin with larger power, a smaller step size is adopted; for the frequency bin with less power, a larger step size is adopted.

Here, α is the adaptation rate, which determines both the convergence speed and equalization performance of the signal PSD dependent algorithm.

$$\mu_{ij,m}{}^{p}(k) = \frac{\alpha}{S_{x,j,m}{}^{p}(k)} \qquad (7.20)$$

7.1.2 Noise PSD directed FD-LMS algorithm

In systems with AWGN channels, the prior error estimation $\mathbf{e}_i(k)$ is made up by two terms: the residual estimated error $\mathbf{r}_i(k)$ and the channel background noise $\boldsymbol{\upsilon}_i(k)$, as shown in (7.21). Since $\mathbf{r}_i(k)$ is linearly dependent on $\mathbf{x}_i{}^{p}(k)$ and independent of $\boldsymbol{\upsilon}_i(k)$, the PSD of $\mathbf{r}_i(k)$ can be estimated by (7.22), which is similar to [35] and [36].

$$\mathbf{e}_{\mathrm{i}}(\mathrm{k}) = \mathbf{r}_{\mathrm{i}}(\mathrm{k}) + \boldsymbol{\upsilon}_{\mathrm{i}}(\mathrm{k}) \tag{7.21}$$

$$\mathrm{S}_{r,\mathrm{i,m}}(\mathrm{k}) = \mathrm{S}_{e,\mathrm{j,m}}(\mathrm{k}) C_{xe,ij,m}{}^{p}(k) \tag{7.22}$$

where $C_{xe,ij,m}{}^{p}(k)$ is the magnitude squared coherence (MSC) function between the input block $\mathbf{X}_{\mathrm{j}}{}^{\mathrm{p}}(\mathrm{k})$ and the prior error block $\mathbf{E}_{\mathrm{i}}(\mathrm{k})$, where the $\mathrm{s}_{ex,\mathrm{ij,m}}{}^{\mathrm{p}}(\mathrm{k})$ is the cross-spectrum density between $\mathbf{X}_{\mathrm{j}}{}^{\mathrm{p}}(\mathrm{k})$ and $\mathbf{E}_{\mathrm{i}}(\mathrm{k})$.

$$C_{xe,ij,m}{}^{p}(k) = \frac{\left|\mathrm{S}_{ex,\mathrm{ij,m}}{}^{\mathrm{p}}(\mathrm{k})\right|^2}{\mathrm{S}_{x,\mathrm{i,m}}{}^{\mathrm{p}}(\mathrm{k})\mathrm{S}_{e,\mathrm{j,m}}(\mathrm{k})} \tag{7.23}$$

Since the MSC function measures the linear relationship between $\mathbf{e}_{\mathrm{j}}(\mathrm{k})$ and $\mathbf{x}_{\mathrm{i}}{}^{\mathrm{p}}(\mathrm{k})$, and $\mathbf{r}_{\mathrm{i}}(\mathrm{k})$ is linearly dependent on $\mathbf{x}_{\mathrm{i}}{}^{\mathrm{p}}(\mathrm{k})$, we can estimate PSD of $\boldsymbol{\upsilon}_{\mathrm{i}}(\mathrm{k})$ as shown in (7.24).

$$\mathrm{S}_{v,\mathrm{j,m}}{}^{\mathrm{p}}(\mathrm{k}) = \mathrm{S}_{e,\mathrm{j,m}}(\mathrm{k})(1 - C_{xe,ij,m}{}^{p}(k)) \tag{7.24}$$

By substituting (7.23) and (7.24) into (7.20), $\mu_{\mathrm{ij,m}}{}^{\mathrm{p}}(\mathrm{k})$ can be estimated by:

$$\mu_{\mathrm{ij,m}}{}^{\mathrm{p}}(\mathrm{k}) = \frac{\alpha}{\mathrm{S}_{\mathrm{x,j,m}}{}^{\mathrm{p}}(\mathrm{k})}\left(1 - \sqrt{1 - \frac{\left|\mathrm{S}_{\mathrm{ex,ij,m}}{}^{\mathrm{p}}(\mathrm{k})\right|^2}{\mathrm{S}_{\mathrm{x,j,m}}{}^{\mathrm{p}}(\mathrm{k})\mathrm{S}_{\mathrm{e,i,m}}(\mathrm{k})}}\right) \tag{7.25}$$

From (7.25), the estimation of $\mu_{\mathrm{ij,m}}{}^{\mathrm{p}}(\mathrm{k})$ relies on the estimation of $\mathrm{S}_{\mathrm{x,j,m}}{}^{\mathrm{p}}(\mathrm{k})$, $\mathrm{S}_{\mathrm{e,i,m}}(\mathrm{k})$, and $\mathrm{S}_{\mathrm{ex,ij,m}}{}^{\mathrm{p}}(\mathrm{k})$. Since $\mathbf{X}_{\mathrm{j}}{}^{\mathrm{p}}(\mathrm{k})$ and $\mathbf{E}_{\mathrm{i}}(\mathrm{k})$ are already known, we can simply estimate $\mathrm{S}_{\mathrm{x,j,m}}{}^{\mathrm{p}}(\mathrm{k})$, $\mathrm{S}_{\mathrm{e,i,m}}(\mathrm{k})$, and $\mathrm{S}_{\mathrm{ex,ij,m}}{}^{\mathrm{p}}(\mathrm{k})$ by the recursively smoothing method as shown from (7.26) to (7.28), where λ is the forgetting factor.

$$\mathbf{S}_{\mathrm{x,j}}{}^{\mathrm{p}}(\mathrm{k}) = \lambda \mathbf{S}_{\mathrm{x,j}}{}^{\mathrm{p}}(\mathrm{k}-1) + (1-\lambda)\left|\mathbf{X}_{\mathrm{j}}{}^{\mathrm{p}}(\mathrm{k})\right|^2 \tag{7.26}$$

$$\mathbf{S}_{\mathrm{e,i}}(\mathrm{k}) = \lambda \mathbf{S}_{\mathrm{e,i}}(\mathrm{k}-1) + (1-\lambda)|\mathbf{E}_{\mathrm{i}}(\mathrm{k})|^2 \tag{7.27}$$

$$\mathbf{S}_{\mathrm{ex,ij}}{}^{\mathrm{p}}(\mathrm{k}) = \lambda \mathbf{S}_{\mathrm{ex,ij}}{}^{\mathrm{p}}(\mathrm{k}-1) + (1-\lambda)\mathbf{X}^{*}{}_{\mathrm{j}}{}^{\mathrm{p}}(\mathrm{k})\mathbf{E}_{\mathrm{i}}(\mathrm{k}) \tag{7.28}$$

According to (7.20) and (7.25), the step size of noise PSD directed method starts from a large value, which makes the faster convergence rate possible; the step size eventually converges to zero, which leads to stable equalization performance with the minimum mean

square error (MSE). Equation (7.20) also shows that, when $s_{v,i,m}^{p}(k)$ equals zero in systems with noise-free channels, the equation becomes the same as (7.7) in the PSD dependent adaptive FD-LMS algorithm.

7.2 Complexity analysis of adaptive noise PSD directed FD-LMS algorithm

In ASIC design, complex multipliers are one of the most resource consuming arithmetic logic in terms of power consumption, area, and cost. Therefore, hardware complexity of the adaptive FD-LMS algorithm can be evaluated by their required number of complex multiplications.

In the M×M adaptive FD-LMS algorithm with block length of 2N, for N equalized output symbols on each of the M modes, the conventional method, the signal PSD dependent method, and the noise PSD directed method all require $4M\cdot(M+1)$ FFT/IFFT processes. In these FFT/IFFT processes, the frequency domain conversion of input blocks requires 2M FFT, the time domain conversion of output blocks consumes M FFT, and frequency domain conversion of prior error blocks needs M FFT. Besides, the gradient and constraint estimation for updating the equalizer needs $4M^2$ FFT. Suppose that radix-2 FFT algorithm is used, $4M\cdot(M+1)$ FFT totally consume $4M\cdot(M+1)\cdot N\cdot \log_2 2N$ complex multiplications for each output symbol.

Apart from FFT, to obtain N output symbols on each of M modes, every adaptive method also requires $2M^2\cdot 2N$ complex multiplications between 2N length input frequency domain blocks and $2M^2$ corresponding equalizers. It also needs $2M^2\cdot 2N$ complex multiplications between M prior error blocks and the conjugate transpose of 2M input frequency domain blocks.

Besides the $8M^2N$ complex multiplications above, the signal PSD dependent method

also requires additional complex multiplications in signal PSD estimation and the update of FDE coefficients. The signal PSD estimation requires 2MN complex multiplications between each input frequency domain block and its conjugate transpose. The update of equalizer's coefficients needs $2M^2 \cdot 2N$ complex multiplications between 2M step size diagonal matrices and M gradient estimation blocks.

Besides the $8M^2N$ complex multiplications, the noise PSD directed algorithm also needs 2MN complex multiplications between each frequency domain input block and its conjugate transpose in signal PSD estimation. It also needs 2MN complex multiplications in the PSD estimation of M prior error blocks and $2M^2 \cdot 2N$ complex multiplications between prior error blocks and conjugate transpose of input frequency domain blocks in cross-correlation estimation of error blocks. The algorithm also additionally needs $2M^2 \cdot 2N$ divisions and $2M^2 \cdot 2N$ square roots. Since the division and square root circuits can be built up with multipliers without lookup tables and other combinational logic [37], we consider these two types of arithmetic logic have the same hardware complexity as complex multipliers for simplicity. So, the noise PSD directed algorithm additionally needs $4MN + 12M^2N$ complex multiplications in total.

According to the above analysis, to obtain N output symbols on each of the M modes, the conventional adaptive FD-LMS algorithm requires $4M \cdot (M+1) \cdot N \cdot \log_2 2N + 8M^2N$ complex multiplications; the signal PSD dependent method requires $4M \cdot (M+1) \cdot N \cdot \log_2 2N + 12M^2N + 2MN$ complex multiplications; the noise PSD directed method requires $4M \cdot (M+1) \cdot N \cdot \log_2 2N + 20M^2N + 4MN$ complex multiplications.

For each output symbol per mode, the required numbers of complex multiplications for the conventional adaptive FD-LMS algorithm, the signal PSD dependent FD-LMS algorithm,

and the noise PSD directed FD-LMS algorithm are $4M\cdot(M+1)\cdot\log_2 2N+8M^2$, $4M\cdot(M+1)\cdot\log_2 2N+12M^2+2M$, and $4M\cdot(M+1)\cdot\log_2 2N+ 20M^2+4M$ respectively.

Specifically, in 6×6 MIMO systems, for each output symbol per mode, the required numbers of complex multiplications for the conventional adaptive FD-LMS algorithm, the signal PSD dependent FD-LMS algorithm, and the noise PSD directed FD-LMS algorithm are $168\cdot\log_2 2N+288$, $168\cdot\log_2 2N+444$, and $168\cdot\log_2 2N+744$, respectively.

7.3 Simulation setup

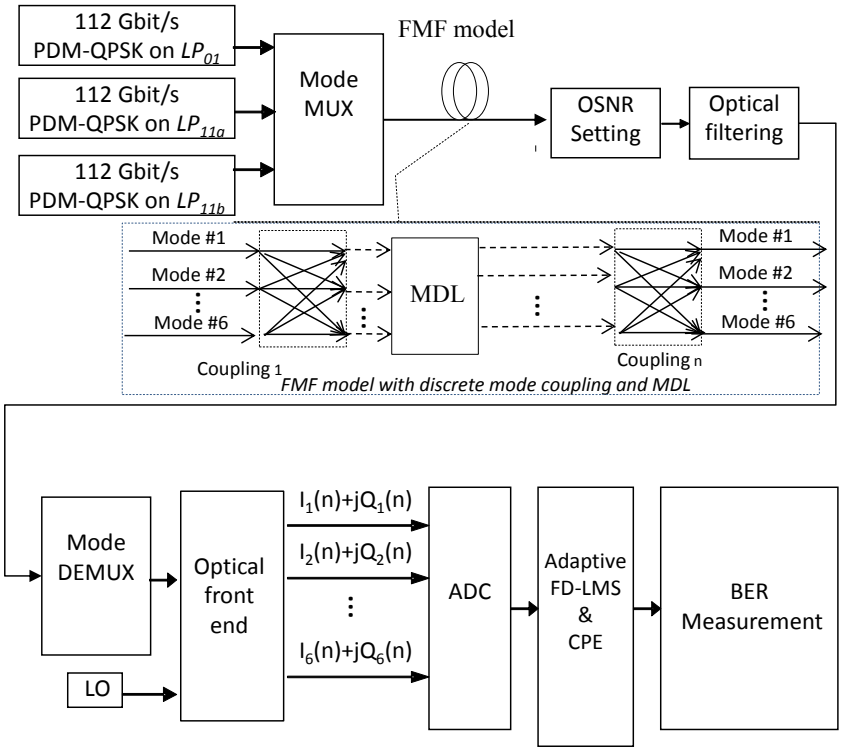

Figure 28. Simulation setup of a six-mode transmission system with 56-Gbit/s QPSK modulated on each mode

A polarization multiplexed three spatial modes (LP_{01}, LP_{11a}, LP_{11b}) transmission system is simulated. The 2^{23}-1 PRBS data sequences are modulated onto each mode in QPSK format at 56 Gbit/s data rate. A mode multiplexer is used to combine the three spatial modes, and a

mode de-multiplexer is used to separate the modes after transmission. -22 dB mode coupling between LP_{01} and LP_{11} modes is assumed at both the mode multiplexer and de-multiplexer [19]. The 6×6 FMF model is similar to the one in [34]. The DMGD is 35 ps/km, and random mode coupling is -34 dB/km with the coupling length of 10 km. The distributed peak-to-peak MDL between LP_{01} group modes and LP_{11} group modes is added after every 80 km transmission. The linewidth of transmitter laser and local oscillator is set to 100 kHz [19]. The fiber loss and chromatic dispersion (CD) are assumed to be completely compensated by the few-mode optical amplifiers and CD compensation modules. The optical noise is added after the FMF transmission, and a Gaussian filter with 33 GHz bandwidth is used to suppress the out-of-band noise before coherent detection.

In DSP, the signal is firstly demodulated by mixing with the local oscillator in optical front end, and then analog-to-digital converter (ADC) re-samples the demodulated signal at two samples per symbol. The conventional adaptive FD-LMS algorithm in [18], the signal PSD dependent adaptive FD-LMS algorithm and the noise PSD directed adaptive FD-LMS algorithm are used for DMGD compensation independently for their convergence speed comparison. The CPE is used together with the adaptive FD-LMS algorithm for the phase recovery of the equalized output blocks. After CPE, the BER and Q factor are calculated.

7.4 Simulation results

Table 2 Computational complexity comparison of conventional FD-LMS, signal PSD dependent, noise PSD directed algorithms at different transmission distance

Transmission distance	Conventional algorithm [18]	PSD dependent algorithm	Noise PSD directed algorithm
1000 km	2304	2460	2760
2000 km	2472	2628	2928
3000 km	2640	2796	3096

Table 2 shows the complexity comparison of three algorithms in terms of needed complex multiplications for each output symbol per mode in six-mode FMF systems. For 1000 km, 2000 km and 3000 km transmission distances, the FD-LMS algorithm requires 2048, 4096 and 8192 FFT sizes for DMGD compensation respectively. It can be seen that, at the 3000 km transmission distance, the noise PSD directed algorithm requires 17.2% and 10.7% more complex multiplications than conventional algorithm and PSD dependent algorithm. If the transmission distance or DMGD is further increased, the growth of hardware complexity of noise PSD directed method gradually decreases and becomes negligible.

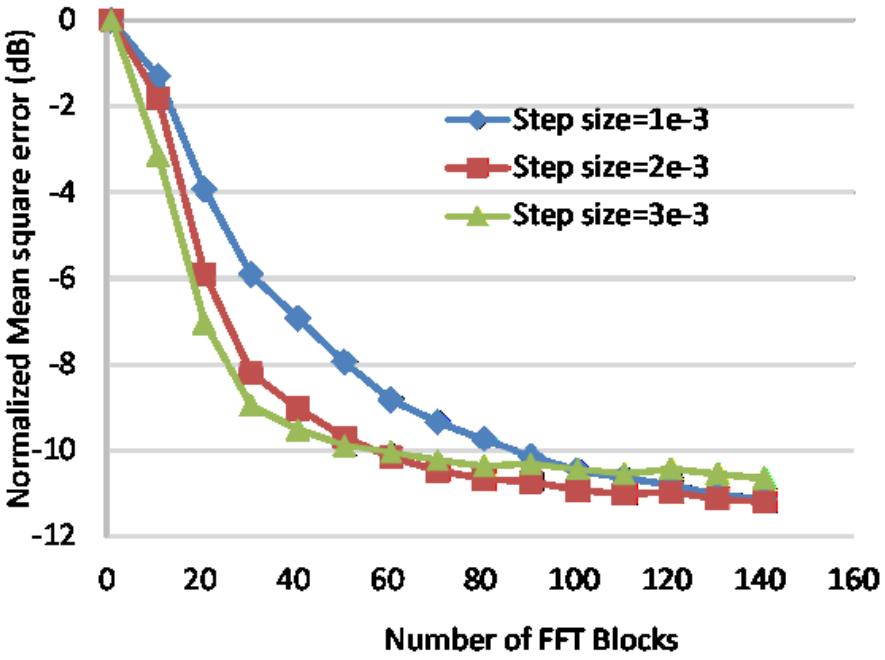

Figure 29. Optimum step size for conventional adaptive FD-LMS algorithm

In order to fairly compare the convergence speed between the conventional adaptive FD-LMS algorithm and the noise PSD directed algorithm, the optimum step size of the

conventional approach is firstly acquired as shown in Figure 29. Although this optimal value is obtained based on the x-polarization of LP_{01} mode, other modes have the same results. The FMF transmission distance is set to 3000 km and OSNR is 14 dB. It can be seen that, when the step size is increased from 0.001 to 0.002, the conventional FD-LMS algorithm converges faster with few MSE degradation. However, when the step size is further increased to 0.003, the equalizer converges to a higher MSE. So, 0.002 is the optimal step size for the conventional method in compensating the DMGD in the 3000 km transmission at 14 dB OSNR.

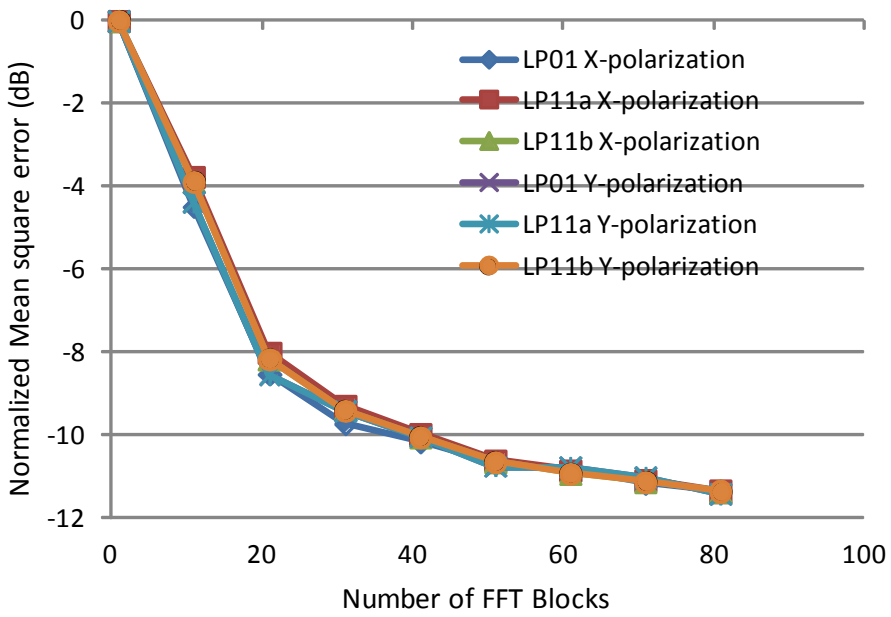

Figure 30. Equalization of signal on all 6 modes with noise PSD directed method

Figure 30 shows the equalization performance of the noise PSD directed method on all 6 modes in a 3000 km transmission at 14 dB OSNR. It can be seen that all 6 modes converge to the same MSE at the same convergence rate.

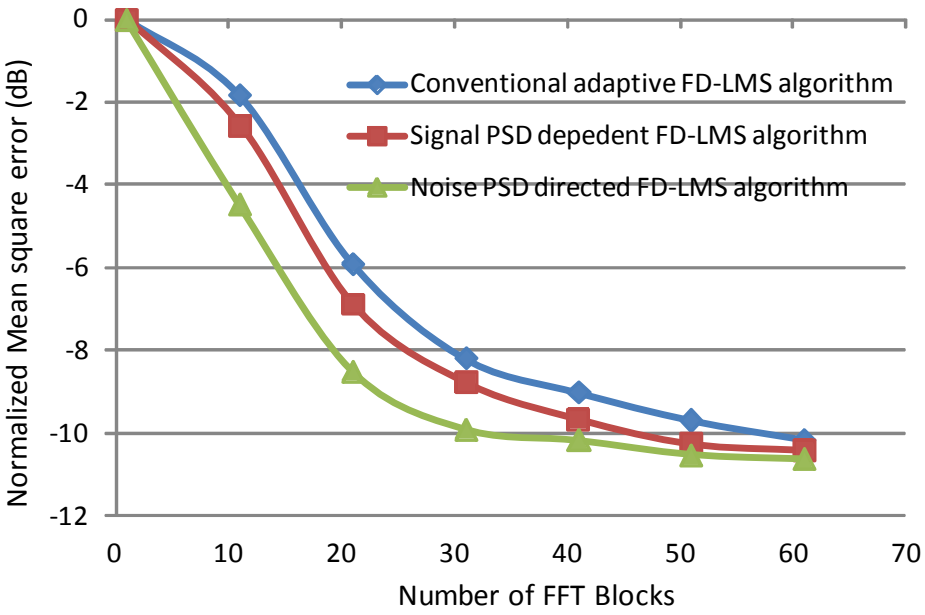

Figure 31. Convergence speed comparison of three adaptive FD-LMS algorithms (mode: LP_{01} X-polarization)

Figure 31 shows the convergence speed comparison of three adaptive FD-LMS algorithms in the 3000 km transmission. OSNR is set to 14 dB. The step size and adaptation rate of the three algorithms are set to the optimal values. From the figure, it can be seen that, to achieve -10 dB normalized MSE (NMSE) (9.5 dB Q-value), the noise PSD directed algorithm only requires 30 blocks while the signal PSD dependent algorithm and the conventional algorithm require 47 and 58 blocks, respectively. The convergence speed is improved by 36.1% and 48.3% respectively. The required large number of blocks not only affects the overall system efficiency by inducing longer overheads, but also may induce additional penalty in systems with the fast-changing channels. Since 30 and 58 FFT blocks are required by the noise PSD dependent method and the conventional method for equalizer convergence and the block length is 8192 samples with 50% overlap, the two algorithms take 4.4 us and 8.5 us to converge respectively. So, the noise PSD dependent method only

requires half of the time for convergence than the conventional algorithm, thus making it more suitable for the FMF systems with the fast-changing channels.

Figure 32 shows the convergence speed comparison between the noise PSD directed algorithm and the signal PSD dependent algorithm at different OSNR levels. The transmission distance is 3000 km, and the FFT size of 8192 is used for DMGD compensation. It can be seen that, when the OSNR is increased from 14 to 22 dB, the improvement of convergence speed is significantly decreased. The result is in accordance with (13), which shows that the noise PSD algorithm has the same convergence speed and equalization performance as the signal PSD dependent approach in the systems with noise-free channels.

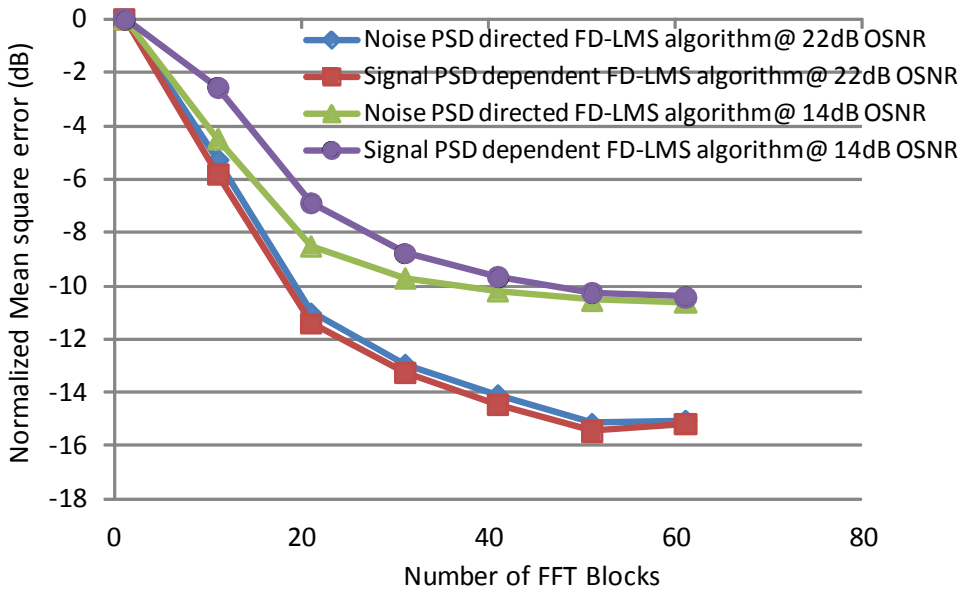

Figure 32. Convergence speed comparison of noise PSD directed algorithm and signal PSD dependent algorithm at different signal OSNR

Figure 33 shows the convergence speed comparison in terms of convergence required number of symbols. The transmission distances are 1000, 2000, and 3000 km, respectively.

The step size and adaptation rate of three algorithms are optimal. The Y-axis is the minimum number of symbols needed to achieve -10 dB NMSE. It can be seen that the system with a longer transmission distance requires a larger number of symbols for the adaptive equalizer convergence. Furthermore, the convergence speed improvement of the noise PSD directed algorithm over other two algorithms is further enhanced in long-haul transmission systems with longer transmission distance. The reason is that, when a larger FFT size is used for DMGD compensation in the systems with longer distance, more frequency bins of the background noise are induced, but the background noise effect can be efficiently mitigated with our new algorithm.

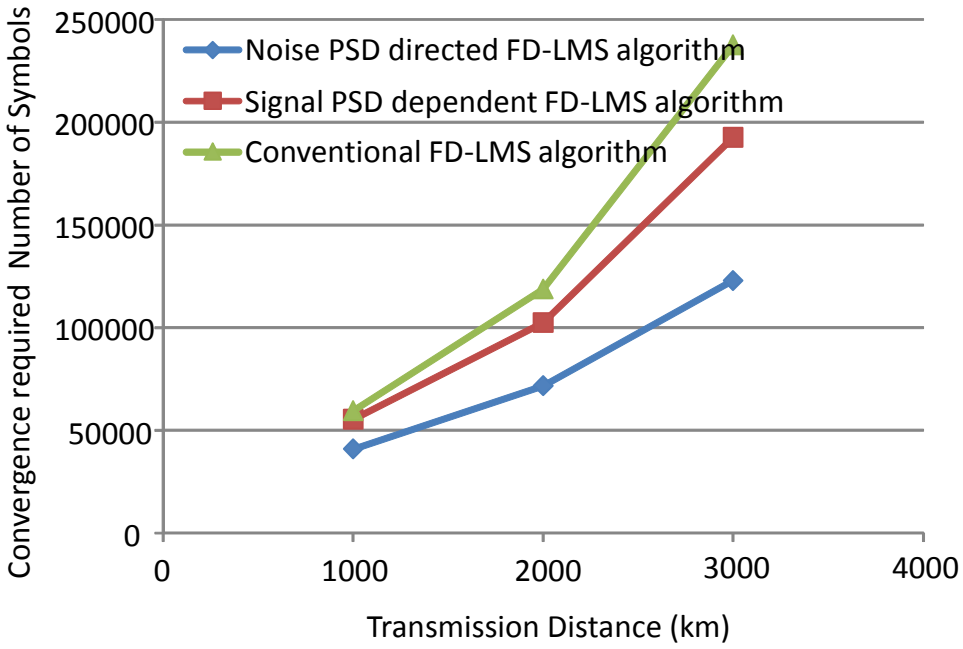

Figure 33. Convergence required number of symbol comparison of three algorithms at different transmission distance

Figure 34 shows the effect of MDL on the noise PSD directed algorithm. The transmission distance is 3000 km, and OSNR is 14 dB. The figure shows that large MDL can induce

significant degradation in equalization performance. It can be seen that the MDL results in more Q penalty on LP_{11a} and LP_{11b} modes than LP_{01} mode. The reason is that the mode coupling between LP_{01} and LP_{11} modes is relatively weak. So, LP_{11} group modes suffer more loss than LP_{01} group modes. If there is strong mode coupling between two mode groups, the equivalent MDL induced the penalty is expected to all spatial modes. The figure also shows that, when the MDL/80 km is increased from 0 to 0.4 dB, the average Q is decreased by 2.2 dB.

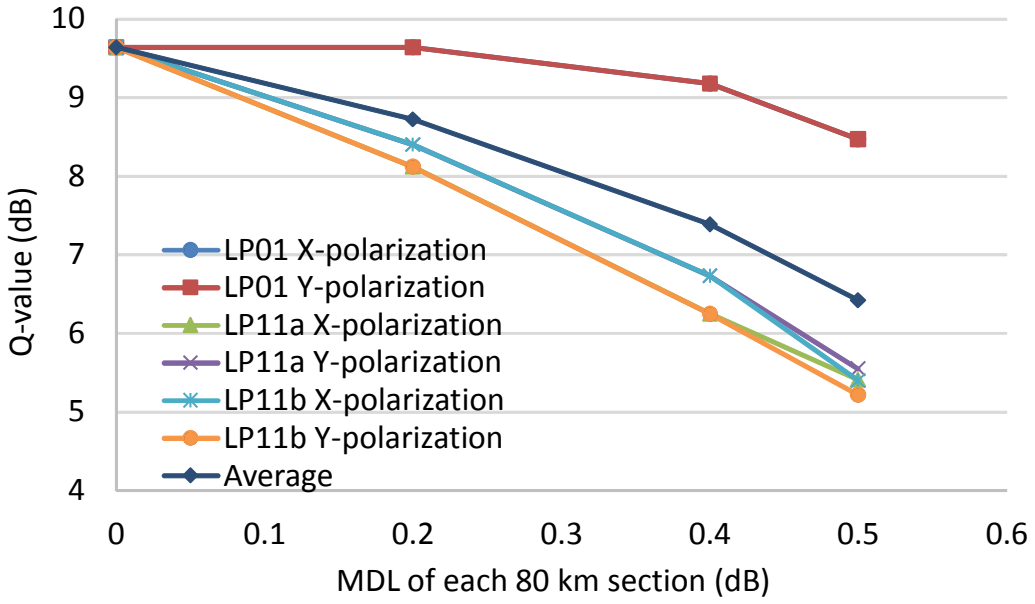

Figure 34. Impact of non-unitary transmission matrix on noise PSD dependent algorithm

Figure 35 shows the convergence speed enhancement of the noise PSD directed method over the other two methods at different MDL per 80 km. The transmission distance is 3000 km and the OSNR is set to 14 dB. It can be seen that, when the MDL/80 km is increased from 0 to 0.4 dB, the noise PSD directed method can keep similar convergence speed

enhancement, which saves 36% and 48% convergence required number of blocks over the signal PSD dependent method and the conventional method, respectively.

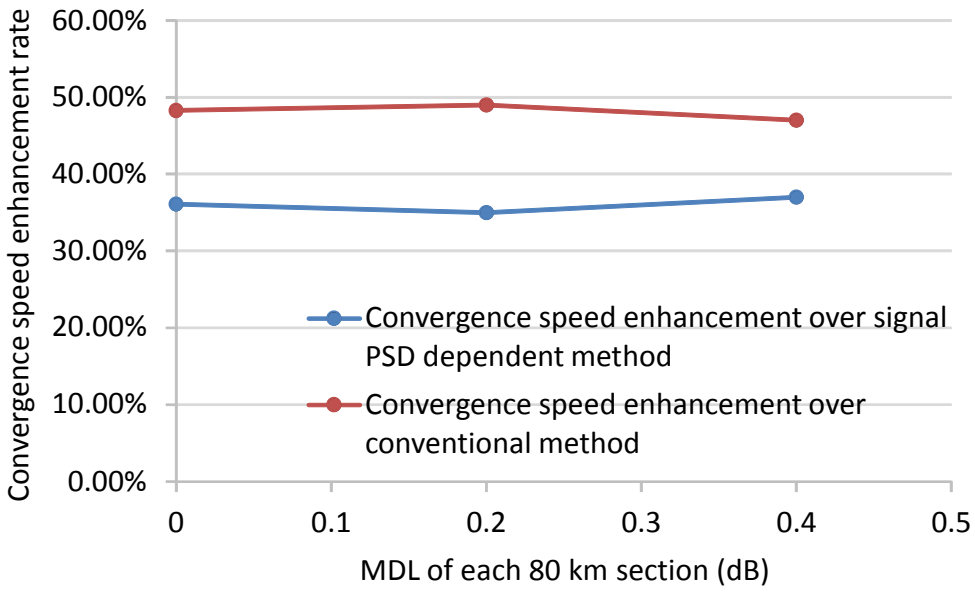

Figure 35. Convergence speed enhancement rate of noise PSD directed method over the other two methods at different MDL

CHAPTER 8: FAST CONVERGENT SINGLE STAGE ADAPTIVE FD-LMS ALGORITHM

8.1 Architecture of fast-convergent single stage equalizer

The architecture of fast convergent single stage equalizer is the same as Figure 27.

8.2 Simulation setup

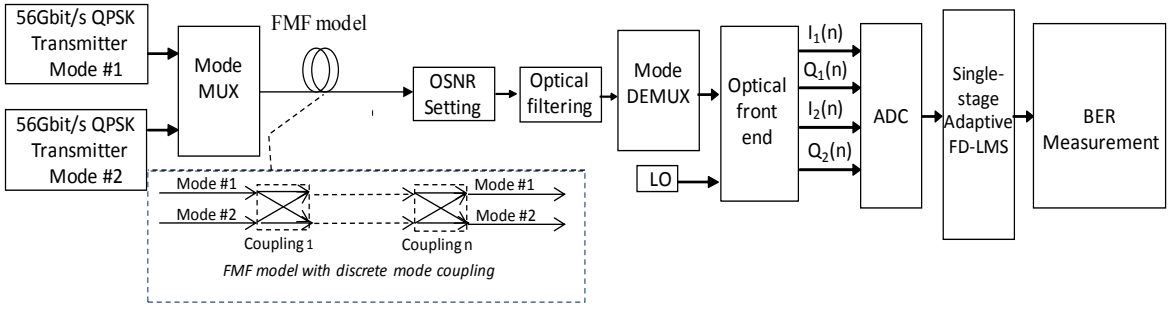

Figure 36. Simulation setup of 112 Gbit/s 2-mode transmission system with single-stage equalizer

Figure 36 shows the simulation setup of an 112 Gbit/s 2-mode transmission system. -8 dB strong mode coupling is induced at both mode multiplexer and de-multiplexer. FMF model is the same as the one in [35], with 35 ps/km DMGD, 20 ps/km CD and -30 dB random mode coupling. Fiber loss is supposed to be compensated with a few-mode amplifier. AWGN is added after FMF transmission, and an optical filter is used to suppress out-of-band noise. In coherent receiver, the signal is firstly re-sample at 2 samples/symbol with analog to digital converter (ADC). The single-stage adaptive FDE using either noise directed FD-LMS algorithm or conventional FD-LMS algorithm is compared for simultaneous CD and DMGD compensation. Bit error rate (BER) and Q-value are estimated after signal equalization.

8.3 Simulation results

Table 3 shows the required number of complex multiplications of both the conventional FD-LMS algorithm and the noise power directed FD-LMS algorithm for accumulated DMGD and CD compensation at different transmission distance. In a 2x2 adaptive FD-LMS algorithm, supposing that minimum FFT size required in adaptive equalization is N and radix-2 FFT algorithm is used, conventional algorithm consumes 12log2N+32 per output symbol on each mode, while noise power directed algorithm consumes 12log2N+88 complex multiplications per output symbol. For 750 km, 1500 km, 3000 km, the required FFT size are 2048, 4096 and 8192, respectively. It can be seen that the noise power directed algorithm need 38% more complex multiplications than conventional FD-LMS algorithm at 3000 km transmission.

Table 3. Computational complexity (number of complex multiplications)

Transmission distance	Conventional algorithm	Noise power directed algorithm
750 km	164	236
1500 km	176	248
3000 km	188	260

Figure 37 shows equalization performance of two adaptive algorithms at different OSNR with 3000 km transmission. It can be seen that both the adaptive noise power algorithm and the conventional algorithm can completely compensate DMGD and CD in FMF.

Figure 38 shows the convergence speed comparison of the noise directed FD-LMS algorithm and the conventional FD-LMS algorithm for compensation 3000 km FMF induced DMGD and CD. At 14 dB OSNR, conventional algorithm requires 51 FFT blocks for convergence to -10 dB

normalized mean square error (NMSE) (10 dB Q-value), while the noise power direct algorithm only requires 25 FFT blocks. At 18 dB OSNR, the conventional method requires 61 FFT block to achieve -13.5 dB NMSE, while the noise power directed method requires only 30 FFT blocks. So, the noise directed algorithm can achieve 51% faster convergence than conventional algorithm.

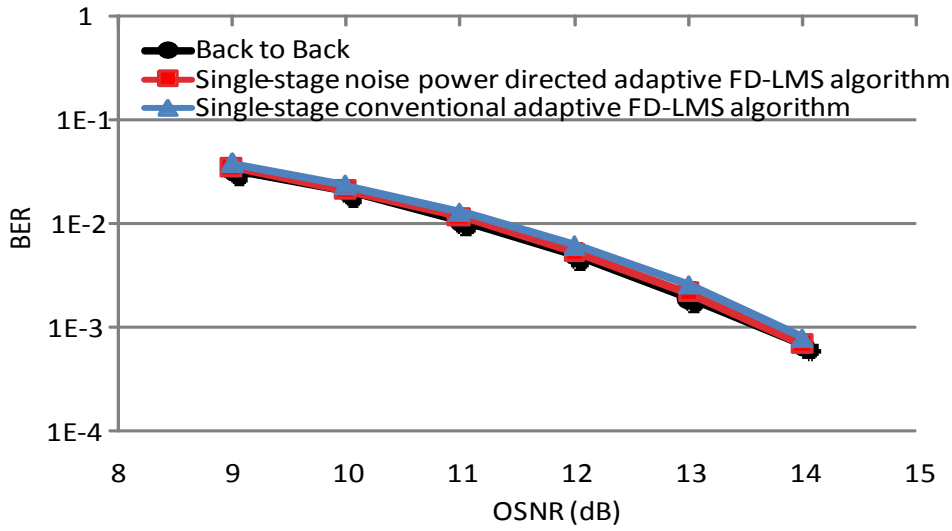

Figure 37. BER vs. OSNR for single-stage adaptive equalizer using noise power direct FD-LMS algorithm and convention FD-LMS algorithm

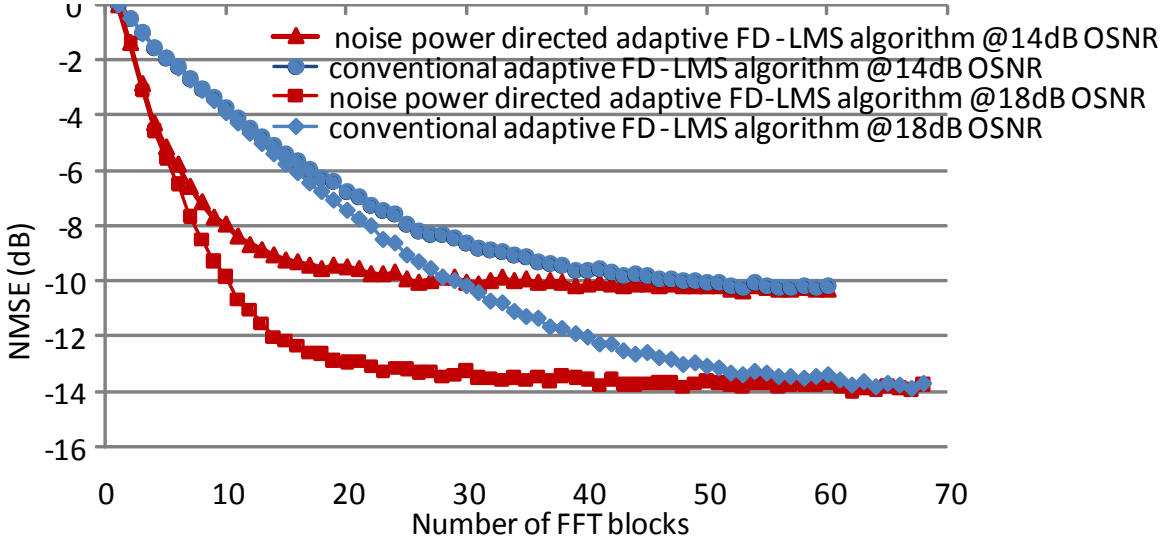

Figure 38. Convergence speed comparison of two single-stage adaptive algorithm at different OSNR setting

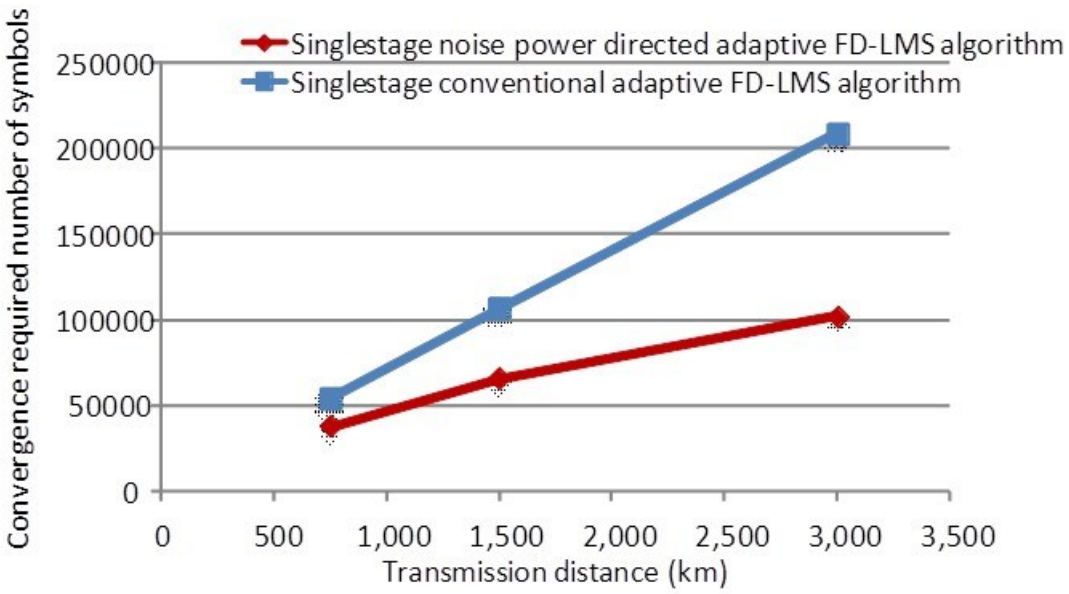

Figure 39. Convergence required number of symbols of two algorithms at different transmission distance

Figure 39 shows that the convergence speed increasing of the noise power directed algorithm over the conventional algorithm is further enhanced in long-haul transmission system with longer distance. The reason for this is that, when larger FFT size required for single-stage equalization in the system with longer distance, more number of frequency bins of background noise are induced, whose effect can be efficiently mitigated with our new algorithm.

CHAPTER 9: CONCLUSION

Space-division-multiplexing (SDM) has been emerging as the next generation technology for cost-effective growth in capacity to keep up with the capacity demand of future Internet. In an SDM system, each independent data channel can be carried by an orthogonal spatial dimension. Several SDM technologies have been proposed and experimentally investigated including bundled SMF, MCF, and FMF. Compared with other technologies, FMF transmission can outperform in terms of fiber cost, leverage of photonic integration device, easy fusion splicing and low nonlinear limit.

However, because of the mode dependent refractive index, a large DMGD can be induced in FMF transmission. Also, because all spatial modes are transmitted in the same physical area, there is inevitable inter-modal crosstalk. When the power of symbols is transferred from one mode to another mode until detection, it causes inter-modal crosstalk. When the power of the symbol is transferred from one mode to another and transferred back, it causes ISI on that spatial channel.

An adaptive MIMO equalizer has been proposed and demonstrated to compensate the DMGD and untangle the crosstalk between the spatial modes using DSP. In M-mode FMF systems, M^2 SISO equalizers are required to build up a M×M MIMO equalizer, in which the required tap length of every SISO equalizer is linearly dependent on the accumulated DMGD. Two adaptive MIMO equalization methods have been proposed for DMGD compensation in FMF systems. RLS method and LMS approach. Compared with RLS approach, LMS algorithm is widely used for it is a good compromise among convergence rate, hardware complexity and equalization performance.

The Adaptive LMS algorithm can either implement in the time domain or in the frequency domain. My results showed that the adaptive FD-LMS algorithm can achieve much lower hardware complexity than TD-LMS algorithm while keeping the same equalization performance.

Except for hardware complexity, the convergence rate of the adaptive equalizer is another important concern. Since the fiber channel is dynamically changing, certain length training sequence needs to be periodically sent during system operation in order to accurately estimate the channel matrix, the length of training sequence is determined by the convergent rate of the MIMO equalizer. If the equalizer converges faster, fewer symbols in the training sequence are needed. However, if the equalizer converges slower, more symbols in the training sequence are required, which will decrease the overall system efficiency.

9.1 Single-stage adaptive MIMO equalizer

In FMF transmission system, except for DMGD, CD is another linear distortion that needs to be compensated in DSP. In conventional fiber transmission systems, a two-stage equalization method is used to compensate the CD by a static FDE in the first stage and compensate DMGD by adaptive FD-LMS in the second stage. However, since the accumulated DMGD is usually much larger than CD in FMF systems, the same adaptive FD-LMS equalizer used for DMGD compensation can also be used for CD compensation without increasing the adaptive equalizer length. Such single-stage equalizer can eliminate the need for an independent CD compensation module, thus can reduce hardware complexity of DSP in FMF transmission systems.

My simulation results showed that the proposed single-stage method can completely compensate the fiber induced CD and DMGD simultaneously while achieving lower hardware

complexity without needs for separate CD compensation module. However, with the conventional adaptive FD-LMS algorithm, the single-stage method may converge slower than the conventional two-stage method. The reason is that the MSE of the proposed single-stage method is larger than two-stage method at the initial convergence, and prior FDE CD compensation of two-stage method decreases the initial MSE.

9.2 Fast-convergent adaptive FD-LMS MIMO equalizer

Two adaptive FDE algorithms were proposed to increase the convergence rate of the conventional adaptive FD-LMS algorithm. One is PSD dependent FD-LMS algorithm, the other one is noise PSD directed FD-LMS algorithm. The simulation results showed that the PSD dependent method is the optimal solution in the system with high OSNR channels, where the frequency bin-wise step size is adopted to make equalization errors converge to zero. The noise PSD directed method can achieve faster convergence speed in the system with low OSNR channels, where the step size of each frequency bin render the equalization error converge to background noise.

The results showed that, in a six-mode 3000 km transmission system with 14 dB OSNR and 35 ps/km DMGD, the noise PSD directed algorithm can increase convergence speed by 48.3% and 36.1% compared with the conventional FD-LMS algorithm and the signal PSD dependent FD-LMS algorithm with 17.2% and 10.7% hardware complexity growth respectively. The simulation results also show that the higher improvement of convergence speed can be achieved in the systems with longer transmission distance or larger DMGD. The proposed algorithm was evaluated at different system MDL. The results showed that, when the MDL per 80 km is increased from 0 to 0.4 dB, the average Q value of all six modes

is decreased by 2.2 dB, while keeping the similar convergence enhancement over other two methods.

Because the uncompensated CD before adaptive MIMO equalizer will decrease its convergence speed, the proposed fast convergent adaptive FD-LMS method is applied to improve the convergence rate of single-stage equalizer. The results showed that the noise PSD directed method can significantly increase the convergence rate of single-stage equalizer. In a 3000 km two-mode transmission system with 35 ps/km DMGD, 20 ps/km/nm CD and 14 dB OSNR, the noise power directed algorithm can converge 51% faster than the conventional adaptive FD-LMS algorithm.

REFERENCES

1. D. J. Richardson, J. M. Fini, and L. E. Nelson, “Space-division multiplexing in optical fibers,” Nature Photonics **7**(5), 354-362 (2013).
2. Sebastian Randel, Roland Ryf, Alberto Sierra, Peter J. Winzer, Alan H. Gnauck, Cristian A. Bolle, René-Jean Essiambre, David W. Peckham, Alan McCurdy, and Robert Lingle, "6×56-Gb/s mode-division multiplexed transmission over 33-km few-mode fiber enabled by 6×6 MIMO equalization," Opt. Express **19**(17), 16697-16707 (2011).
3. S. Randel, R. Ryf, A. Gnauck, M. A. Mestre, C. Schmidt, R. Essiambre, P. Winzer, R. Delbue, P. Pupalaikis, A. Sureka, Y. Sun, X. Jiang, and R. Lingle, "Mode-Multiplexed 6×20-GBd QPSK Transmission over 1200-km DGD-Compensated Few-Mode Fiber," in Optical Fiber Communication Conference, OSA Technical Digest (Optical Society of America, 2012), paper PDP5C.5.
4. Roland Ryf, Sebastian Randel, Alan H. Gnauck, Cristian Bolle, Alberto Sierra, Sami Mumtaz, Mina Esmaeelpour, Ellsworth C. Burrows, René-Jean Essiambre, Peter J. Winzer, David W. Peckham, Alan H. McCurdy, and Robert Lingle, "Mode-Division Multiplexing Over 96 km of Few-Mode Fiber Using Coherent 6 × 6 MIMO Processing," J. Lightwave Technol. **30**(4), 521-531 (2012).
5. A. Li, A. Al Amin, X. Chen, and W. Shieh, "Reception of Mode and Polarization Multiplexed 107-Gb/s CO-OFDM Signal over a Two-Mode Fiber," in Optical Fiber Communication Conference/National Fiber Optic Engineers Conference OSA Technical Digest (Optical Society of America, 2011), paper PDPB8.

6. Neng Bai, Ezra Ip, Yue-Kai Huang, Eduardo Mateo, Fatih Yaman, Ming-Jun Li, Scott Bickham, Sergey Ten, Jesús Liñares, Carlos Montero, Vicente Moreno, Xesús Prieto Vincent Tse, Kit Man Chung, Alan Pak Tao Lau, Hwa-Yaw Tam, Chao Lu, Yanhua Luo, Gang-Ding Peng, Guifang Li, and Ting Wang, "Mode-division multiplexed transmission with inline few-mode fiber amplifier," Opt. Express **20**(3), 2668-2680 (2012).
7. R. Ryf, N. K. Fontaine, M. A. Mestre, S. Randel, X. Palou, C. Bolle, A. H. Gnauck, S. Chandrasekhar, X. Liu, B. Guan, R. Essiambre, P. J. Winzer, S. Leon-Saval, J. Bland-Hawthorn, R. Delbue, P. Pupalaikis, A. Sureka, Y. Sun, L. Grüner-Nielsen, R. V. Jensen, and R. Lingle, "12 x 12 MIMO Transmission over 130-km Few-Mode Fiber," in Frontiers in Optics/Laser Science XXVIII, OSA Technical Digest (Optical Society of America, 2012), paper FW6C.4.
8. V. Sleiffer, Y. Jung, V. Veljanovski, R. van Uden, M. Kuschnerov, Q. Kang, L. Grüner-Nielsen, Y. Sun, D. Richardson, S. Alam, F. Poletti, J. Sahu, A. Dhar, H. Chen, B. Inan, T. Koonen, B. Corbett, R. Winfield, A. Ellis, and H. De Waardt, "73.7 Tb/s (96X3x256-Gb/s) mode-division-multiplexed DP-16QAM transmission with inline MM-EDFA," in European Conference and Exhibition on Optical Communication, OSA Technical Digest (Optical Society of America, 2012), paper Th.3.C.4.
9. Ezra Ip, Ming-Jun Li, Kevin Bennett, Yue-Kai Huang, Akihiro Tanaka, Andrey Korolev, Konstantin Koreshkov, William Wood, Eduardo Mateo, Junqiang Hu, and Yutaka Yano, "146λ × 6 × 19-Gbaud Wavelength-and Mode-Division Multiplexed Transmission Over 10 × 50-km Spans of Few-Mode Fiber With a Gain-Equalized Few-Mode EDFA," J. Lightwave Technol. **32**(4), 790-797 (2014).

10. Peter J. Winzer and Gerard J. Foschini, "MIMO capacities and outage probabilities in spatially multiplexed optical transport systems," Opt. Express **19**(17), 16680-16696 (2011).
11. L. Gruner-Nielsen, Y. Sun, J. W. Nicholson, D. Jakobsen, R. Lingle, and B. Palsdottir, "Few Mode Transmission Fiber with low DGD, low Mode Coupling and low Loss," in Optical Fiber Communication Conference, OSA Technical Digest (Optical Society of America, 2012), paper PDP5A.1.
12. S. Arik, D. Askarov and J. Kahn, "Adaptive Frequency-Domain Equalization in Mode-Division Multiplexing Systems," J. Lightwave Technol **32**(99), 1-13 (2014).
13. N. Bai and G. Li, "Adaptive frequency-domain equalization for mode-division multiplexed transmission," IEEE Photon. Technol. Lett. **24**(21), 1918 -1921 (2012).
14. S. Arik, J. M. Kahn and K.-P. Ho "MIMO signal processing in mode-division multiplexing," IEEE Signal Process. Mag. **31**(2), 25-34 (2014).
15. N. Bai and G. Li, "Adaptive frequency domain equalization for mode-division multiplexed transmission," in Proceeding of IEEE Photonic. Society. Summer Topical Conference (IEEE, 2012), pp.185 -186.
16. S. S. Haykin, *Adaptive Filter Theory, 3rd edition* (Prentice Hall, 2001).
17. O. Z. Chahabi, R. L. Bidan, M. Morvan, and C. Laot, "Efficient Frequency-Domain Implementation of Block-LMS/CMA Fractionally Spaced Equalization for Coherent Optical Communications," IEEE Photon. Technol. Lett, **23**(22), 1-6 (2014).
18. Md. Saifuddin Faruk and Kazuro Kikuchi, "Adaptive frequency-domain equalization in digital coherent optical receivers," Opt. Express **19**(13), 12789-12798 (2011).

19. Neng Bai, Cen Xia, and Guifang Li, "Adaptive frequency-domain equalization for the transmission of the fundamental mode in a few-mode fiber," Opt. Express **20**(21), 24010-24017 (2012).
20. N. Bai, E. Ip, M. Li, T. Wang, and G. Li, "Experimental demonstration of adaptive frequency-domain equalization for mode-division multiplexed transmission," in Optical Fiber Communication Conference/National Fiber Optic Engineers Conference, OSA Technical Digest (Optical Society of America, 2013), paper OM2C.5.
21. S. Randel, M. A. Mestre, R. Ryf, and P. Winzer, "Digital Signal Processing in Spatially-Multiplexed Coherent Communication," in European Conference and Exhibition on Optical Communication, OSA Technical Digest (Optical Society of America, 2012), paper Tu.3.C.1.
22. X. He, X. Zhou, Y. Weng, and Z. Pan, "Low Complexity Single-Stage Adaptive Frequency Domain Equalizer for SDM Systems using Few Mode Fibers," in Advanced Photonics, OSA Technical Digest (Optical Society of America, 2013), paper SPT4D.2.
23. Z. Pan ; Xuan He and Yi Weng" Hardware efficient frequency domain equalization in few-mode fiber coherent transmission systems," Proc. SPIE 9009, 900906 (2013).
24. X. He, X. Zhou, J. Wang, Y. Weng, and Z. Pan, "A Fast Convergence Frequency Domain Least Mean Square Algorithm for Compensation of Differential Mode Group Delay in Few Mode Fibers," in Optical Fiber Communication Conference/National Fiber Optic Engineers Conference, OSA Technical Digest (Optical Society of America, 2013), paper OM2C.4.

25. X. He, Y. Weng, J. Wang, and Z. Pan, "Noise Power Directed Adaptive Frequency Domain Least Mean Square Algorithm with Fast Convergence for DMGD Compensation in Few-Mode Fiber Transmission Systems," in Optical Fiber Communication Conference, OSA Technical Digest (Optical Society of America, 2014), paper Th3E.1.
26. Xuan He, Yi Weng and Zhongqi Pan, "A Step-Size Controlled Method for Fast Convergent Adaptive FD-LMS Algorithm in Few-Mode Fiber Communication Systems," J. Lightwave Technol (to be published).
27. Nokia Simens, Space Division Multiplexing: A new milestone in the evolution of fiber optic communication, White paper.
28. D. Gloge, "Weakly Guiding Fibers," Appl. Opt. **10**(10), 2252-2258 (1971).
29. Junyi Wang, Digital Signal Processing in Coherent Optical Communications 2013, 99 pages; 3590082.
30. E. Ip, J. M. Khan, "Feedforward Carrier Recover for Coherent Optical Communications," J. Lightwave Technol **27**(13), 2675-2692 (2009).
31. S. Randel, "Space Division Multiplexed Transmission," in Optical Fiber Communication Conference/National Fiber Optic Engineers Conference, OSA Technical Digest (Optical Society of America, 2013), paper OW4F.1.
32. Arik, S.O., Kahn, J.M., Keang-Po Ho, "MIMO Signal Processing for Mode-Division Multiplexing: An overview of channel models and signal processing architectures," Signal Processing Magazine, IEEE **31**(2), 25-34 (2014).
33. K. Shi, and X. Ma, "A Frequency Domain Step-Size Control Method for LMS Algorithms," IEEE Signal Processing Letters **17**(2), 125-128 (2010).

34. J. Vuong, P. Ramantanis, A. Seck, D. Bendimerad, and Y. Frignac, "Understanding Discrete Linear Mode Coupling in Few-Mode Fiber Transmission Systems," in European Conference and Exposition on Optical Communications, OSA Technical Digest (Optical Society of America, 2011), paper Tu.5.B.2.
35. J. Leibrich and W. Rosenkranz, "Frequency Domain Equalization with Minimum Complexity in Coherent Optical Transmission Systems," in Optical Fiber Communication Conference, OSA Technical Digest (Optical Society of America, 2010), paper OWV1.
36. K. Shi, X. Ma, and G. T. Zhou, “A residual echo suppression technique for nonlinear acoustic echo cancellation,” in Proceeding of IEEE Conference on Acoustics, Speech, and Signal Processing (IEEE, 2008), pp. 267 - 260.
37. E. M. Schwarz, M. J. Flynn, “Using a Floating-Point Multiplier’s Internals for High-Radix Division and Square Root,” Technical Report, 1993.

Xuan He. Bachelor of Science, Xian University of Post and Telecommunications, Spring 2009; Master of Science, University of Louisiana at Lafayette, Spring 2013; Doctor of Philosophy, University of Louisiana at Lafayette, Fall 2014
Major: Computer Engineering
Title of Dissertation: MIMO Digital Signal Processing in Few-Mode Fiber Optical Communication Systems
Dissertation Director: Dr. Zhongqi Pan
Pages in Dissertation: 87; Words in Abstract: 288

ABSTRACT

Space-division multiplexing (SDM) has been extensively proposed to overcome the next capacity crunch with ever-increasing data and video traffic. Among several SDM approaches, mode-division-multiplexing (MDM) in few-mode fiber (FMF) is the most auspicious technology. One key challenge in FMF transmission systems is random mode coupling among different fiber modes, which can cause severe inter-modal crosstalk. Moreover, large accumulated differential mode group delay (DMGD) can induce significant inter-symbol interference (ISI).

The approach of adaptive multi-input multi-output (MIMO) digital signal processing (DSP) has been proposed and demonstrated to untangle the crosstalk between the spatial modes and compensate the DMGD. In FMF systems, compared with time-domain adaptive MIMO signal processing, the implementation of frequency domain method achieves much lower hardware complexity. In this dissertation, a single-stage adaptive MIMO equalizer is proposed to compensate both DMGD and chromatic dispersion (CD) simultaneously in order to further reduce the hardware complexity.

Except for hardware complexity, the convergence rate of adaptive MIMO equalizer is another essential concern. The adaptive MIMO equalizer with slower convergence speed

requires longer training symbols, thus decreasing the system overall efficiency. In the dissertation, two advanced step size control methods are presented to increase the convergence rate of the conventional FD-LMS algorithm. The first approach is the signal power spectral density (PSD) dependent method, which adopts the step size for each frequency bin inverse to its power level in order to converge the estimated equalization error to zero, thus it is the optimal solution in the systems with noise-free channel. The other method is the noise PSD directed method, which adopts the frequency bin-wise step size to render the estimated error converge to the channel background noise, thus it is the optimum solution in the systems with additive white Gaussian noise channel.

Biographical Sketch

Xuan He was born in Xi'an, Shaanxi, China, May 23th, 1987. He received his B.S from Xian University of Post and Telecommunications, Xi'an, in China in 2009. He started his doctoral studies at the University of Louisiana at Lafayette, in the Fall of 2009. He had two summer internships at Juniper Networks, CA and one summer collaboration in AT&T Lab-Research, New Jersey. His dissertation focused on MIMO Digital Signal Processing in Few-Mode Fiber Optical Communication Systems. He served as a reviewer for Optics Express and he was an IEEE and OSA student member.